

Open clusters: III. Fundamental parameters of B stars in NGC 6087, NGC 6250, NGC 6383 and NGC 6530.

B type stars with circumstellar envelopes.*

Y. Aidelman^{1,2,**}, L. S. Cidale^{1,2,***}, J. Zorec^{3,4}, and J. A. Panei^{1,2,***}

¹ Instituto de Astrofísica La Plata, CCT La Plata, CONICET-UNLP, Paseo del Bosque S/N, B1900FWA, La Plata, Argentina.

² Departamento de Espectroscopía, Facultad de Ciencias Astronómicas y Geofísicas, Universidad Nacional de La Plata (UNLP), Paseo del Bosque S/N, B1900FWA, La Plata, Argentina.

³ Sorbonne Université, UPMC Univ. Paris 06, 934 UMR7095-IAP, 75014 Paris, France.

⁴ CNRS, 934 UMR7095-IAP, Institut d’Astrophysique de Paris, 98bis Bd. Arago, 75014 Paris, France.

Received / Accepted

ABSTRACT

Context. Stellar physical properties of star clusters are poorly known and the cluster parameters are often quite uncertain.

Aims. Our goals are to perform a spectrophotometric study of the B star population in open clusters to derive accurate stellar parameters, search for the presence of circumstellar envelopes and discuss the characteristics of these stars.

Methods. The BCD spectrophotometric system is a powerful method to obtain stellar fundamental parameters from direct measurements of the Balmer discontinuity. To this end, we wrote the interactive code MIDE3700. The BCD parameters can also be used to infer the main properties of open clusters: distance modulus, color excess and age. Furthermore, we inspect the aspect of the Balmer discontinuity to put in evidence the presence of circumstellar disks and identify Be-star candidates. An additional set of high resolution spectra, in the H α region, is used to confirm the Be nature of these stars.

Results. In this work we provide T_{eff} , $\log g$, M_v , M_{bol} and spectral types for a sample of 68 stars in the field of the open clusters NGC 6087, NGC 6250, NGC 6383, and NGC 6530, as well as the cluster distances, ages and reddening. Then, based on a sample of 230 B stars in the direction of the eleven open clusters studied along these three series of papers, we report new six Be stars, four blue straggler candidates, and fifteen B type stars (called Bdd) with a double Balmer discontinuity which indicates the presence of circumstellar envelopes. We discuss the distribution of the fraction of B, Be and Bdd star cluster members per spectral subtype. The majority of the Be stars are dwarfs and present a maximum at the spectral type B2-B4 in young and intermediate-age open clusters (< 40 Myr). Another maximum of Be stars is observed at the spectral type B6-B8 in open clusters older than 40 Myr, where the population of Bdd stars also becomes relevant. The Bdd stars seem to be in a “passive” emission phase.

Conclusions. Our results support previous statements that the Be phenomenon is present along the whole main sequence band and occurs in very different evolutionary states. We find clear evidence of an enhance of stars with circumstellar envelopes with cluster age. The Be phenomenon reaches its maximum in clusters of intermediate-age (10 – 40 Myr) and the number of B stars with circumstellar envelopes (Be plus Bdd stars) keeps also high for the older clusters (40 – 100 Myr).

Key words. open clusters and associations: individual (NGC 6087); individual (NGC 6250); individual (NGC 6383); individual (NGC 6530); stars: fundamental parameters; stars: emission-line

1. Introduction

This is the third of a series of papers devoted to the spectroscopic study of a total of 230 B-type stars in the field of view of eleven open clusters. This study is based on the spectrophotometric BCD (Barbier-Chalonge-Divan) system, developed by Barbier & Chalonge (1939) and Chalonge & Divan (1973).

Our main goals were to derive accurate stellar parameters (T_{eff} , $\log g$, M_v , M_{bol} and spectral types) of the B star population in open clusters and search for the presence of B stars with cir-

cumstellar envelopes. A secondary objective was to provide an improved set of cluster parameters and identify their star memberships.

Particularly, this work presents a spectrophotometric investigation of 68 B-type stars in the region of the galactic clusters NGC 6087, NGC 6250, NGC 6383, and NGC 6530. The results related with other seven clusters were published by Aidelman et al. (2012, 2015, hereafter Paper I and Paper II, respectively). In addition, all of the information gathered along this series of papers allows us to analyze here the relative frequency of cluster star members per spectral subtypes and age, the distribution of stars with circumstellar envelopes in a $T_{\text{eff}} - \log g$ diagram and discuss some characteristics of the peculiar group of Be stars. In Paper I, we introduced the BCD method as a tool to evaluate precise physical parameters of the cluster’s stars and the cluster properties, in a fast and direct way, by measuring the Balmer discontinuity (BD). On the other hand, as the BCD parameters are

Send offprint requests to: Y. Aidelman e-mail: aidelman@fcaglp.unlp.edu.ar

* Observations taken at CASLEO, operating under agreement of CONICET and the Universities of La Plata, Córdoba and San Juan, Argentina

** Fellow of CONICET, Argentina

*** Member of the Carrera del Investigador Científico, CONICET, Argentina

not affected by interstellar absorption and/or circumstellar emission/absorption (Zorec & Briot 1991), the location of stars in the Hertzsprung-Russell (HR) diagram is more accurate than classical methods based on plain photometry, thus allowing for better determinations of cluster ages. Moreover, the BCD method also enables us to characterize each star in very crowded stellar regions with fundamental parameters that cannot be strongly perturbed by the light of the nearest objects, so that it is possible to discuss properly their cluster membership by taking color excesses and distance estimates, as done in Paper II.

Another advantage of the study of the BD is that it allows us to recognize B stars with circumstellar envelopes since some B-type stars display a second component of the BD (called hereafter SBD. For more details see Divan 1979; Zorec & Briot 1991; Cidale et al. 2001; Zorec et al. 2005; Cidale et al. 2007, and Paper I). The main BD, in absorption, occurs as in normal dwarf stars and is attributed to the central star. The SBD is situated at shorter wavelengths and is originated in an envelope having low pressure (Divan 1979). A SBD in absorption is often related with spectral line “shell” signatures, while a SBD in emission is generally accompanied by line emission features. We can then use the SBD, when is present, as a criterion to detect stars having circumstellar envelopes or disks. This is possible even though they do not exhibit clear signs of emission or shell-absorption features among the first attainable members of the Balmer lines, as a consequence of a late B spectral type or the low resolution of the available spectrophotometric spectra. Therefore, as a complement of this work, we present spectra of B stars in open clusters that exhibit a SBD and discuss the properties of this star population (see details in sections §5.2 and 5.3).

The paper is organized as follow: data acquisition and reduction procedure are given in section § 2. In section § 3 we briefly describes the BCD method and its application to our star sample. Spectrophotometric results on the cluster parameters (NGC 6087, NGC 6250, NGC 6383, and NGC 6530) and their memberships are given in section § 4. In section § 5 we analyze the relative frequency of B and Be stars per spectral subtypes and age, using data of the eleven open clusters studied. We discuss the derived stellar parameters and the presence of circumstellar envelopes in the late B-type stars. Our conclusions are summarized in section § 6.

2. Observations

Low-resolution spectra of additional 68 B-type stars in four open clusters were obtained in long slit mode during multiple observing runs between 2003 and 2013 with a Boller & Chivens spectrograph¹ attached to the J. Sahade 2.15 m telescope at the Complejo Astronómico El Leoncito (CASLEO), San Juan, Argentina. The log of observations is listed in Table 1. The spectra were taken with a Bausch and Lomb replica diffraction grating of 600 l mm⁻¹ (#80, blazed at 4000 Å) and slit widths of 250 μm and 350 μm oriented along east-west. The slit widths were set to match an aperture on the sky of about 2'3 and 3'3, respectively, according to the average seeing at CASLEO.

Before 2011, we used a PM 512 CCD detector covering the spectral wavelength range of 3500 – 4700 Å. The rest of the

¹ The optical layout of this instrument is similar to the Boller & Chivens spectrograph offered for the du Pont 100-inch telescope of Las Campanas Observatory (Chile), <http://www.lco.cl/telescopes-information/irenee-du-pont/instruments/website/boller-chivens-spectrograph-manuals/user-manual/the-boller-and-chivens-spectrograph>

observations were carried out with the CCD detector TEK 1024 that covered the wavelength interval 3500–5000 Å. The effective spectral resolutions are 4.53 Å and 2.93 Å every two pixels ($R \sim 900$, $R \sim 1400$), respectively. A comparison lamp of He-Ne-Ar was taken after each science stellar spectrum.

The observations were performed at the lowest possible zenith distance to minimize refraction effects due to the Earth's atmosphere and, thus, to avoid light losses as a function of wavelength. For an air mass of 1.5 the expected differential refraction effect between 4000 Å and 6000 Å is 1'08 (<http://www.eso.org/sci/observing/tools/calendar/ParAng.html>). This assures that the light-loss is minimized. Each night we observed at least two flux standard stars (HR 3454, HR 5501, HR 7596, HR 4468 and HR 5694) to perform the spectral flux calibrations.

The reduction procedure (overscan, bias, trimming, and flat-field corrections) was carried out with the IRAF² software package (version 2.14.1) and all spectra were wavelength calibrated and corrected for atmospheric extinction. We used the atmospheric extinction coefficients published in CASLEO web-page (<http://www.casleo.gov.ar/info-obs.php>).

An addition set of high-resolution spectra ($R = 12600$) were taken with the echelle spectrograph REOSC in the spectral range 4225 – 6700 Å to seek the H α emission in the B stars with a SBD. These observations were done only for some of the star members identified in the eleven studied Galactic clusters (see Table 2). The instrumental configuration was a 400 l mm⁻¹ grating (#580), a 250 μm slit width and a TK 1K CCD detector. A Th-Ar comparison lamp was used to apply the wavelength calibration.

3. Methodology

As was previously described in Papers I and II, we derived from low-resolution spectroscopic data the fundamental parameters of open clusters and individual stars using the BCD spectrophotometric method.

For each star of our sample we measured the BCD parameters: λ_1 , D , and Φ_b (or Φ_{bb}). The first two parameters describe the average spectral position and the height of the BD, respectively. The third parameter is the color gradient that measures the slope of the Paschen continuum. Then using the BCD calibrations (see Paper I) we obtain the stellar fundamental parameters: spectral type, luminosity class, effective temperature (T_{eff}), logarithm of surface gravity ($\log g$), absolute visual magnitude (M_v), absolute bolometric magnitude (M_{bol}) and intrinsic color gradient (Φ_b^0).

To perform all these measurements, one of us (YA) wrote the interactive code MIDE3700³, in *Python* language. Its name corresponds to the Spanish acronym for *Medición Interactiva de la Discontinuidad En 3700 Å* (Interactive Discontinuity Measurement at 3700 Å). With this tool the user can work over the stellar spectrum and choose the best fits to Balmer and Paschen continua. The code then automatically delivers the values of D , λ_1 and Φ_b and the corresponding fundamental parameters of a star.

From observed and intrinsic color gradients we estimated the color excess, $E(B - V) = 2.1(\Phi_b - \Phi_b^0)$ or $E(B - V) = 2.3(\Phi_{bb} - \Phi_{bb}^0)$, of each star and its distance modulus, using

² IRAF is distributed by the National Optical Astronomy Observatory, which is operated by the Association of Universities for Research in Astronomy (AURA), Inc., under cooperative agreement with the National Science Foundation

³ The authors gently offer the code MIDE3700 to whom wish to use it.

the apparent visual magnitude available in the literature. In addition, we calculated the stellar luminosity ($\mathcal{L}_*/\mathcal{L}_\odot$), stellar mass (M_*/M_\odot) and age of each star interpolating in the stellar evolutionary models, for a non-rotating case and $Z = 0.014$, provided by Ekström et al. (2012). For more details see Paper II.

From these data we derived for each open cluster, the true distance modulus, $(m_v - M_v)_0$, the color excess $E(B - V)$ and the age, with their respective error bars. The distance modulus and memberships are calculated using an iterative procedure as explained in Paper II, based on the statistical distribution of individual distance modulus for the observed full sample of stars in the direction of each cluster. The first step is the calculation of a mean distance modulus (DM^0) and its standard deviation (σ^0). Then, we select a smaller sample that consist of stars with distance moduli at $1\sigma^0$ of DM^0 . With this reduced sample we recalculate new values, which are the adopt mean true distance modulus of the cluster $DM_c = (m_v - M_v)_0$ and its standard deviation σ . The color excesses $E(B - V)$ are calculated using the same small sample.

The membership criterion is then based on the distance modulus of each star and its error bars. When this distance modulus is outside the region defined by 3σ size around the mean cluster distance modulus, the star is considered a non-member (*nm*). If the star is inside a region between 2σ and 3σ size, the star is considered a probable non-member (*pnm*). If the star is between 1σ and 2σ size it is a probable member (*pm*) and if its distance modulus is less than 1σ size the star is considered as member (*m*).

On the other hand, cluster membership probabilities, p , of individual stars can be estimated using the statistical P-method approach. Assuming the null hypothesis is true, if the P-value is less than (or equal to) a given significance level, α , then the null hypothesis is rejected instead if the P-value is large it is accepted. As we are dealing with a rather modest number of objects in each cluster, to define a well distribution of distances we adopt the standard statistical level of significance of 5% to classify a star as a cluster member.

The cluster age was estimated from the HR diagram by setting the isochrones (Ekström et al. 2012) to the locations of the stars classified as members and probable members of the cluster. These stars are identified as *m* and *pm* in column 5 of Tables 10, 12, 14, and 16.

4. Results

For each cluster analyzed here: NGC 6087, NGC 6250, NGC 6383, and NGC 6530, we present a brief summary of previous studies and the results obtained with the BCD system of each individual star. This information is listed in two tables. The first table shows the star identification, the observed BCD parameters D , λ_1 , Φ_b and the stellar physical properties (spectral type and luminosity class, T_{eff} , $\log g$, M_v , M_{bol} , and the intrinsic color gradient Φ_b^0). The BCD spectral types have been tested, when it was possible, with those of the standard MK system. In some occasions we were not able to interpolate or extrapolate the BCD parameters because they were out of the range of the BCD calibrations. In those cases we used the MK-classification system to derive the spectral types and the corresponding fundamental parameters (Cox & Pilachowski 2000). In addition, the intrinsic color gradients were estimated using the relation between Φ_b and $(B - V)$ given by Moujtahid et al. (1998).

The second table includes for each star: the visual apparent magnitude m_v , the obtained color excess $E(B - V)$, the true distance modulus $(m_v - M_v)_0$, the angular distance to the cluster

center AD , the membership probability p , the luminosity \mathcal{L}_* relative to the solar one, the stellar mass M_* (in unit of solar mass), and the age. The coordinates of the cluster and their angular diameters were taken from Dias et al. (2002).

The cluster parameters are presented and discussed in the following subsections.

4.1. NGC 6087

NGC 6087 ($\alpha = 16^{\text{h}} 18^{\text{m}} 50$ and $\delta = -57^\circ 56^{\text{m}} 1$; J2000) is located near the southern edge of the Normae constellation in a region that appears to be uniformly reddened near the Galactic plane (Sagar & Cannon 1997). It is one of the brightest open clusters in this region and it is very rich in Be stars. Several authors studied this cluster and its parameters were estimated with different techniques. In Table 3 we can notice that the $E(B - V)$ values range from 0.13 mag to 0.22 mag and the cluster distance modulus is between 9.375 mag and 10.233 mag ($750 \text{ pc} < d < 1000 \text{ pc}$). The cluster age presents big uncertainties, ranging from 10 – 20 Myr to 146 Myr.

The spectral classification of the stars in the region of NGC 6087 was performed only by Feast (1957) who reported the $H\beta$ line in emission in the star No. 10. Additional Be stars (Nos. 9, 14, and 22) were reported by Mermilliod (1982), while the star No. 25 was classified as a CP2 star by Maitzen (1985) using the photometric Δa -system.

Although some preliminary stellar parameters for this cluster were previously reported by Aidelman et al. (2010), here we provide an improved set of BCD measurements (see Tables 9 and 10) that were obtained using the MIDE3700 code and the new BCD M_v -calibration given by Zorec & Briot (1991), instead of that reported by Zorec (1986). From these data we obtained the following cluster parameters: $(m_v - M_v)_0 = 9.00 \pm 0.19$ mag, $d = 629 \pm 54$ pc and $E(B - V) = 0.35 \pm 0.03$ mag. As we derived a large value of $E(B - V)$ our distance modulus is slightly lower than those previously reported in the literature. We attribute this large $E(B - V)$ to particularities of the selected sample. Apart of the fact that many of the stars of the sample present evidence of circumstellar envelopes, the large $E(B - V)$ excess could be attained to the non uniform dust distribution (see Fig. 1), revealed in the WISE (Wide-field Infrared Survey Explorer, Wright et al. 2010) band-3 image, where we identified our sample.

Considering our criterion for selecting star members (see section § 3), based on $(m_v - M_v)_0 = 9.00$ mag and $\sigma = 0.5$ mag, we find 12 star members (*m*, Nos. 1, 8, 9, 10, 11, 13, 14, 15, 25, 36, 128, 156). Furthermore, taking into account the p values, we can confirm that the stars Nos. 8, 9, 13, 14, 25 and 128 are cluster members (see Table 10), and stars Nos. 33 and 35 are non-member (*nm*).

On the other hand, according to the calculated angular distances and considering that the mean cluster diameter is $14'$ (Dias et al. 2002), the most distant stars are Nos. 1 and 22.

In the literature we found that stars reported as *pnm* and/or *nm* are Nos. 7, 10, and 129 (Landolt 1964; Schmidt 1980; Turner 1986). However, as both Nos. 7 and 10 are Be stars (see section § 5), these authors could have been underestimated the absolute magnitudes due to the presence of the circumstellar envelope. From proper motion measurements Dias et al. (2014) classified stars Nos. 7, 8, 9, 10, 11, 13, 14, 15, 25, 128, 129, 156, as members and assigned to the star No. 35 a probability of 11 %.

Our studied sample of stars defined well the cluster HR diagram over which we had plotted the isochrones for non-rotating star models given by Ekström et al. (2012, see Fig. 2). The Be star No. 22, classified as *pm*, is the most luminous object in the

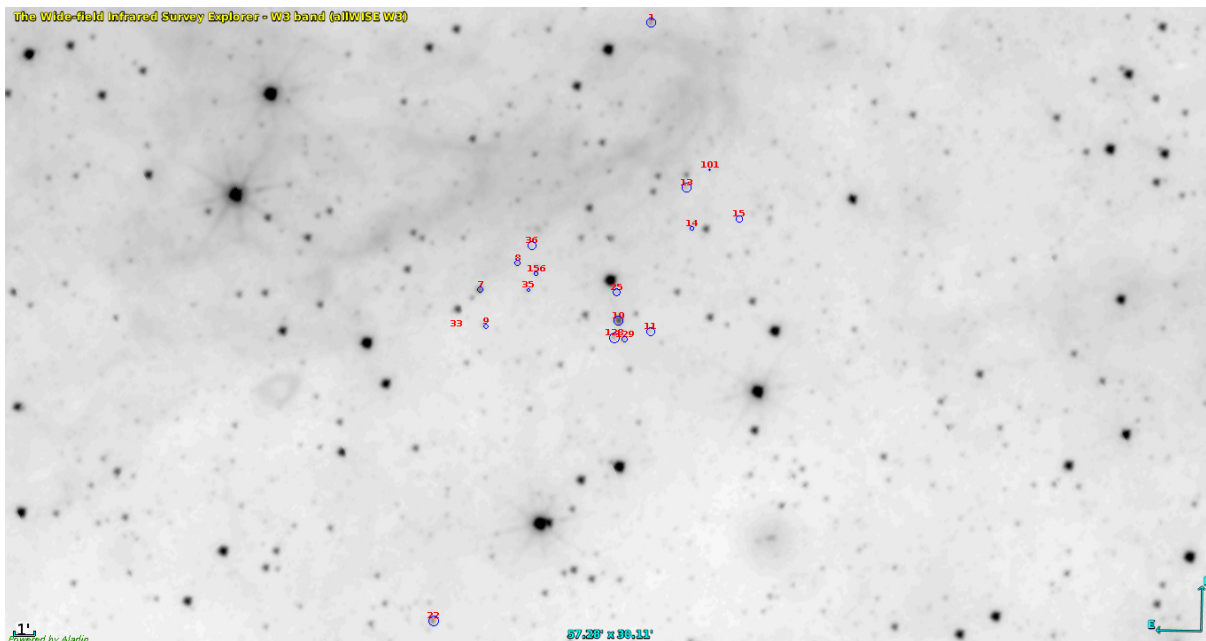


Fig. 1. NGC 6087: WISE band 3 image showing a non uniform dust distribution. The circles indicate the positions of the stars which are proportional to the measured $E(B - V)$.

Table 3. NGC 6087: Previous and current determinations of color excess, distance, and age.

Reference	$E(B - V)$ [mag]	$(m_v - M_v)_0$ [mag]	d [pc]	age [Myr]
Trumpler (1930) ^{sp}	870	...
Fernie (1961) ^{ph}	0.22	9.4	750	10 – 20
Landolt (1963) ^{ph}	0.20	9.8 ± 0.1
Breger (1966) ^{ph}	0.20 ± 0.01	9.7
Graham (1967) ^{ph}	...	9.9	950	...
Lindoff (1968) ^{sc}	930	~ 41
Becker & Fenkart (1971) ^{ph}	0.13	9.96	820	...
Tosi (1979) [*]	55 ± 5 ; 55 ± 9.6 ; 146 ± 11
Schmidt (1980) ^{ph}	0.17 ± 0.01 **	9.60 ± 0.09
Janes & Adler (1982) ^{ph}	0.21	10.23	...	~ 40
Turner (1986) ^{ph}	...	9.78 ± 0.13	902 ± 10	...
Sagar (1987) ^{ph,sp}	0.18 ± 0.05	9.8	...	20
Meynet et al. (1993) ⁱ	~ 71
Sagar & Cannon (1997) ^{ph}	0.22	...	1000 ± 100	65
Robichon et al. (1999) ^h	769	...
Rastorguev et al. (1999) ^h	820	...
Baumgardt et al. (2000) ^h	819.67	...
Loktin & Beshenov (2001) ^h	...	9.375	...	~ 95
Kharchenko et al. (2005) ^h	901	~ 85
Piskunov et al. (2007) ^h	0.18
An et al. (2007) ^{ph}	0.132 ± 0.007	9.708 ± 0.048
This work	0.35 ± 0.03	9.00 ± 0.19	629 ± 54	~ 55

Notes. ^(h) Results based on HIPPARCOS data. ⁽ⁱ⁾ Results based on the isochrone fitting method. ^(ph) Results based on photometric data. ^(sc) Results based on synthetic clusters. ^(sp) Results based on spectroscopic data. ^(*) The age of the cluster was derived by three different methods: isochrone fitting, position of the turn-off point, and period of Cepheid stars (55 Myr, 146 Myr and 55 Myr, respectively). The author argued that the most accurate method is the isochrone fitting followed by the Cepheid periods. ^(**) The color excess $E(B - V)$ was calculated in this work, using the $E(b - y)$ value given by Schmidt (1980) and the relation $E(b - y) = 0.74 E(B - V)$.

HR diagram and is located in the most external region of the cluster (see Fig. 1). This star was also classified as a blue straggler. Therefore, if we do not consider this object in the sample,

the inferred cluster age is ~ 55 Myr. This value agrees very well with those obtained by Tosi (1979).

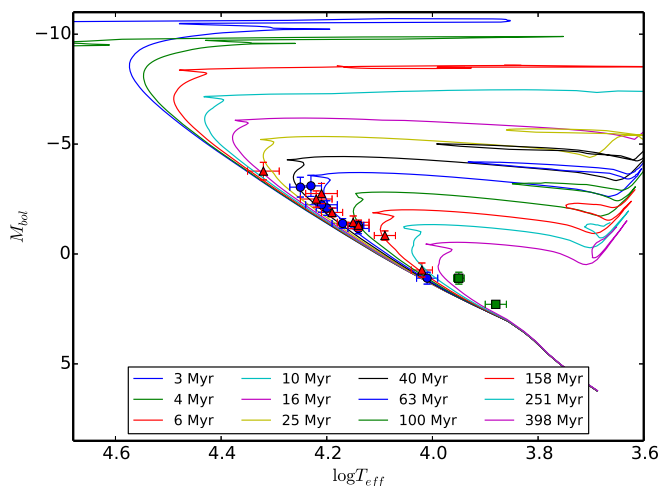


Fig. 2. NGC 6087: HR diagram. The estimated age for this cluster is ~ 55 Myr. The isochrone curves are given by Ekström et al. (2012). Members and probable members of the clusters are denoted in \bullet (blue) symbols and probable non-members and non-members in \blacksquare (green). Star members with circumstellar envelope are indicated in \blacktriangle (red).

The BCD spectral types agree with the spectral classification reported by Feast (1957), considering the sample of stars that are in common. In addition, we have determined the spectral type of four stars (Nos. 25, 33, 101, and 128) for the first time. In our sample we distinguish seven stars showing a SBD: Nos. 7, 9, 10, 11, 14, 101, and 156 (see Fig. 12 and 13).

4.2. NGC 6250

NGC 6250 ($\alpha = 16^{\text{h}} 57^{\text{m}} 58$ and $\delta = -45^{\circ} 56^{\text{m}} 6$; J2000) has a peculiar distribution in the sky. The cluster consists of a very compact central region surrounded by sparse bright stars. Several arguments suggest that the cluster is associated with a prominent dust cloud and is affected by differential reddening. Feinstein et al. (2008) identified several dust components along the light of sight and found that most of the stars do not show indications of intrinsic polarization.

Previous cluster parameters were estimated with different techniques (see Table 4) and they show a low scatter. The spectral classification of its individual members was performed by Herbst (1977) and a detailed chemical analysis of 19 upper main-sequence stars was done by Martin et al. (2017). Star No. 35 is the only known Be star, star No. 34 was reported as peculiar (in He and in the K-line, Lodén & Nordström 1969) and star No. 3 as a visual binary (Herbst 1977).

The results obtained from MIDE3700 code are listed in Tables 11 and 12. From them we derived the mean cluster parameters: $(m_v - M_v)_0 = 10.55 \pm 0.33$ mag, $E(B - V) = 0.38 \pm 0.16$ mag and $d = 1288 \pm 210$ pc. The obtained color excess is in very good concordance with those determined by Moffat & Vogt (1975) and Herbst (1977). Figure 3 is an image obtained with WISE in the band 3 that shows the dust distribution around the open cluster NGC 6250. The distance modulus agrees better with the determination done by Piskunov et al. (2008).

From our membership criterion we found 8 members (Nos. 1, 2, 3, 17, 18, 35, 37 and HD 329 211) based on $(m_v - M_v)_0 = 10.55$ mag and $\sigma = 0.9$ mag. Among them, stars Nos 1, 2 17, 35, 37 and HD 329 211 are confirmed members with their p values (see Table 12). Stars Nos. 21, 22, 33, 34,

and CD-49 11096 are pm , star No. 32 is a probable non-member (pnm). Star No. 4 is nm (it has a low p value) but it was reported as pnm by Moffat & Vogt (1975).

Our membership criterion agrees with the memberships derived from polarimetric measurements (Feinstein et al. 2008) and from proper motion determinations (Dias et al. 2014), in relation with those stars observed in common (Nos. 1, 2, 3, 17, 18).

An inspection of the angular distances of the stars respect to the cluster center reveals that half of them are located out of the mean angular diameter assumed for the cluster (of $10'$, Dias et al. 2002). Since the stars Nos. 33, 34, and 35 are m or pm according to our membership criterion, one might think that the angular diameter of the cluster is larger than $10'$. Extreme cases are CD-49 11096 and HD 329 211. We have not found any information regarding the memberships of these stars in the literature.

On the other hand, according to our HR diagram the cluster age is ~ 6 Myr (see Fig. 4) which is lower than the values reported in the literature (see Table 4). To justify older ages with our data (by factors 2 or 4) we had to admit that we are overestimating effective temperatures by nearly 60% that correspond to underestimations of the Balmer discontinuity of the order of 0.1 dex which is impossible to admit. The age discrepancy we find is quite significant and could be due to the early star sample considered by the different authors to identify the isochrone that determines the cluster age. In our work, to derive the age of the cluster we used stars of spectral type B0, while Herbst (1977) and Battinelli & Capuzzo-Dolcetta (1991) used stars of spectral type B1, instead Kharchenko et al. (2005) and McSwain & Gies (2005) took a sample of stars of spectral type B2. These spectral types imply $(T_{\text{eff}}, \log L/L_{\odot})$ parameters that range from (4.48, 4.63) to (4.47, 4.89) for stars B0V to B0III, (4.43, 4.24) to (4.41, 4.53) for stars B1V to B1III and (4.35, 3.73) to (4.32, 4.1) for stars B2V to B2III. These $(T_{\text{eff}}, \log L/L_{\odot})$ -intervals identify isochrones in Fig. 4 near 6 Myr, 16 Myr and 25 Myr, respectively, which correspond to the estimated ages by the different authors marked in Table 4.

The BCD spectral classification agrees with that done by Herbst (1977) for eight of the twelve stars we have in common. Furthermore, we have derived for the first time a spectral classification for CD-49 11096. Only the star No. 1 presents a SBD in its spectrum, which is in emission (see Fig. 13). This star has a high effective temperature ($T_{\text{eff}} \approx 27\,400$ K). From simple arguments based on the opacity of circumstellar envelopes of Be stars it is not possible to have conspicuous continuum emissions in the Balmer continuum near $\lambda 3600 \text{ \AA}$ without some emission in the first members of the Balmer series. The line emission in such classical Be stars is rarely very high. Unfortunately, the BCD spectrophotometric observations of this star did not extend up to the $H\beta$ line. On the other hand, the spectroscopic observation done with REOSC shows H absorption line profiles (see section §5.3), although low and high resolution observations are not simultaneous. Therefore, the star was classified as Bdd.

Finally, we confirm that No. 34 is peculiar and we classified it as a He-strong star. The star shows very intense lines of He I. We measured the following equivalent widths: $EW_{4471} = 1.9 \text{ \AA}$, $EW_{4387} = 1.3 \text{ \AA}$, $EW_{4026} = 2.1 \text{ \AA}$, which are about twice greater than the ones expected at the spectral type B0V (see Didelon 1982).

4.3. NGC 6383

NGC 6383 ($\alpha = 17^{\text{h}} 34^{\text{m}} 48$ and $\delta = -32^{\circ} 34^{\text{m}} 0$; J2000) is a rather compact open cluster which could be part of the Sgr OB1

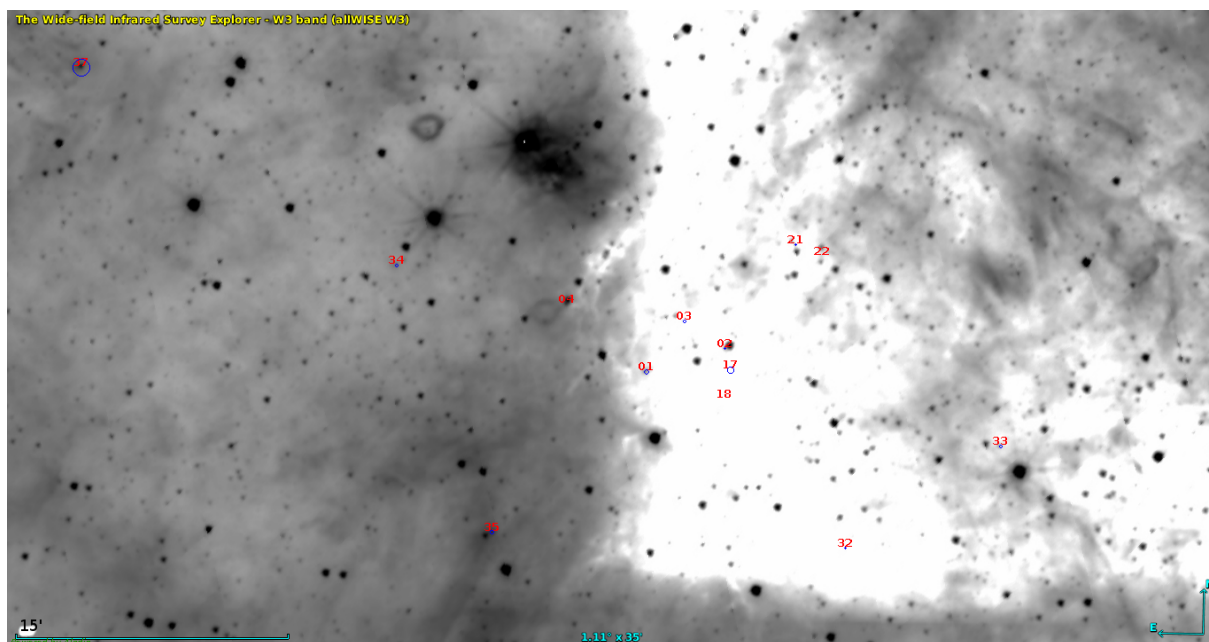


Fig. 3. Idem Fig. 1 but for NGC 6250. Stars HD 329 211 and CD-49 11096 are not included due to its large angular distance from the center of the cluster.

Table 4. NGC 6250: Previous and current determinations of color excess, distance, and age.

Reference	$E(B - V)$ [mag]	$(m_v - M_v)_0$ [mag]	d [pc]	age [Myr]
Moffat & Vogt (1975) ^{ph}	0.38 ± 0.02	9.92^*	950	...
Herbst (1977) ^{ph}	0.37	10.05	...	14
Battinelli & Capuzzo-Dolcetta (1991) ^c	~ 14
Kharchenko et al. (2005) ^h	865	~ 26
McSwain & Gies (2005) ^{ph}	0.35^{**}	9.69	...	~ 26
Piskunov et al. (2008) ^h	0.35	10.77
This work	0.38 ± 0.16	10.55 ± 0.33	$1\,288 \pm 210$	~ 6

Notes. ^(c) Results based on catalogs. ^(h) Results based on HIPPARCOS data. ^(ph) Results based on photometric data. ^(*) The intrinsic distance modulus was calculated in this work, using $(m_v - M_v)$ and $E(B - V)$ values published by Moffat & Vogt (1975) with $R_v = 3.1$. ^(**) The color excess $E(B - V)$ was calculated in this work, using the $E(b - y)$ value given by McSwain & Gies (2005) and the relation $E(b - y) = 0.74 E(B - V)$.

association together with NGC 6530 and NGC 6531 (cf. Rauw & De Becker 2008). The brightest star HD 159 176 is a well studied X-ray double-line spectroscopic binary responsible for the ionization of the H II region RCW 132.

This cluster was widely studied with different techniques (see Table 5). In contrast to other studied clusters, the spectral classification of the star members was done by several authors (The 1966; Antalová 1972; Lloyd Evans 1978; The et al. 1985; van den Ancker et al. 2000). This cluster has many Be and peculiar stars: Nos. 1 and 100 were reported as double-line spectroscopic binaries (Trumpler 1930; Sahade & Berón Dávila 1963, respectively) while Nos. 14 and 83 were reported as possible spectroscopic binaries (Lloyd Evans 1978). No. 3 was reported as an Ap spectroscopic variable (The et al. 1985; Landstreet et al. 2008). Stars Nos. 1 and 6 were classified as blue stragglers and, in particular, No. 1 was also classified as a emission line star. The star No. 76 was reported to have H α in emission.

Tables 13 and 14 list the derived stellar parameters, and from them we infer the following cluster parameters: $(m_v - M_v)_0 = 9.61 \pm 0.38$ mag, $E(B - V) = 0.51 \pm 0.03$ mag and $d = 834 \pm 158$ pc. The derived color excess is larger than previous published val-

ues, therefore our distance estimate is lower. We attribute this high value to the special characteristics of the selected sample (most of the stars have circumstellar envelopes and are located in a dense dusty region, see Fig. 5).

Considering the values $(m_v - M_v)_0 = 9.61$ mag and $\sigma = 1.13$ mag we classified 8 star members (Nos. 1, 2, 10, 14, 57, 76, 83, and 100), 2 as *pm* (Nos. 3 and 6) and 2 as *pnm* (Nos. 47 and 85, both are the coolest stars of this sample). Stars Nos. 1, 2, 14, 76, and 83 are also members according to our p-method criterion. Star No. 85 was reported as *nm* by Lloyd Evans (1978). The stars classified as *m* and *pm* also present *AD* lower than the cluster angular diameter (of 20', Dias et al. 2002). Moreover, based on proper motion measurements, stars Nos. 1, 2, 3, 6, 10, 14, 47, 57, 83, 100 were considered members by Dias et al. (2014) while star No. 85 has a 1% of probability. Then we have 1 star in discrepancy with Dias et al. (2014, No. 47).

The cluster HR diagram is very well defined and the derived cluster age, ~ 3 Myr, agrees with the most of the values found in the literature (Fitzgerald et al. 1978; Battinelli & Capuzzo-Dolcetta 1991; Kharchenko et al. 2005; Paunzen et al. 2007). However, if we consider that the star No. 6 has started to evolve

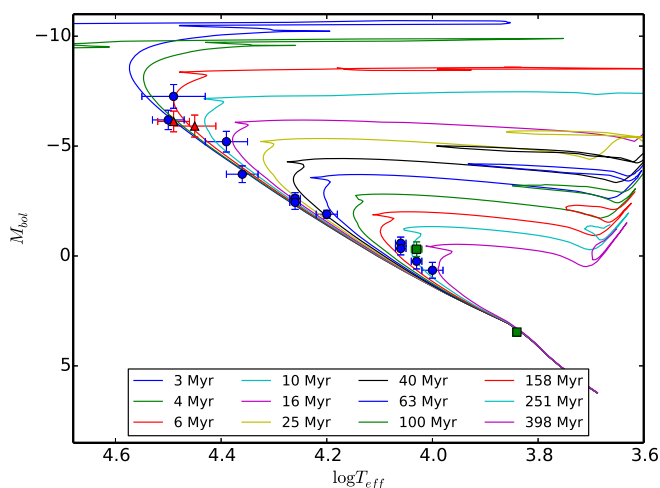


Fig. 4. NGC 6250: HR diagram. The estimated age for this cluster is ~ 6 Myr. The isochrone curves are given by Ekström et al. (2012). Members and probable members of the clusters are denoted in \bullet (blue) symbols and probable non-members and non-members in \blacksquare (green). Star members with circumstellar envelopes are indicated in \blacktriangle (red).

(see Fig. 6, second more bright star of the sample) and accept that the X-Ray Be binary star No. 1 (HD 159 176) is a blue straggler, then the age of the cluster is between 6 Myr and 10 Myr.

Our spectral classification agrees with that done in previous works, in particular with Lloyd Evans (1978). We observed a SBD in absorption in the spectrum of the star No. 57 (see Fig. 13).

4.4. NGC 6530

NGC 6530 ($\alpha = 18^{\text{h}} 04^{\text{m}} 31$ and $\delta = -24^{\circ} 21^{\text{m}} 5$; J2000) is a very young cluster located in the H II region M8, also known as the Lagoon Nebulae, near the Sagittarius-Carina spiral Galactic arm. Several authors studied this cluster and its parameters were estimated with different techniques (see Table 6). The color excess $E(B - V)$ and the cluster distance have large uncertainties, with values between 0.30 mag and 0.541 mag, and between 730 pc and 1900 pc, respectively. However the cluster age is better defined, being it less than 7 Myr.

The spectral classification of the individual star members was performed by Walker (1957); Hiltner et al. (1965); Chini & Neckel (1981); Torres (1987); Boggs & Bohm-Vitense (1989), and Kumar et al. (2004). The cluster has many variable stars and many emission line stars. Stars Nos. 7, 9, 56, 65, 86, and 100 were reported as spectroscopic binaries, and Nos. 43 and 73 as triple systems. In addition, stars Nos. 42, 45, 56, 60, 65, and 100 show H lines in emission, however, it is still debating if these emissions originate in the H II region or in a circumstellar envelope. On the other hand, Kumar et al. (2004) reported the star No. 65 as a Herbig Ae/Be I or III, and Niedzielski & Muciek (1988) classified the stars No. 59 as an unknown peculiar type and No. 66 as a He-weak. Finally, stars Nos. 73 and 93 were reported as blue stragglers.

With the BCD system we derive the stellar fundamental parameters (Tables 15 and 16) and the mean cluster parameters: $(m_v - M_v)_0 = 11.76 \pm 0.20$ mag, $E(B - V) = 0.26 \pm 0.05$ mag and $d = 2245 \pm 215$ pc. The distance modulus agree very well with the determination done by Lindoff (1968), but our derived color excess is systematically lower than previous published values.

Figure 7 illustrates the WISE band 3 image in the surroundings of NGC 6530 together with our color excess determinations. The low $E(B - V)$ values we derived indicate that the dusty region is located behind the cluster.

Taking into account our membership criterion (with $(m_v - M_v)_0 = 11.76$ mag and $\sigma = 0.78$ mag) we found 15 members (Nos. 32, 42, 43, 56, 60, 61, 65, 66, 68, 70, 73, 76, 86, 93, and 100), 6 *pm* (Nos. 7, 9, 45, 55, 59, and 85) and 2 *nm* (No. 80 and LSS 4627). We can confirm as cluster members the stars Nos. 43, 65, 70, and 86 because they have large p values. On the other hand, LSS 4627 is the star farthest from the center of the cluster and we considered it as a *nm*. The rest of stars have angular distances lower than the cluster angular diameter of $14'$ (Dias et al. 2002). We have 17 stars in common with Dias et al. (2014, Nos. 32, 42, 43, 55, 56, 59, 60, 61, 65, 66, 68, 70, 73, 76, 80, 86, 93.) who considered all of them as members. Therefore, only the star No. 80 is in discrepancy.

Even though, the stars show some scatters in the HR diagram (probably due to the binary nature of many of them), the cluster age seems to be about 4 – 6 Myr (see Fig. 8). This value agrees with most of the previous determination.

Our spectral classification confirms that done by Hiltner et al. (1965); Chini & Neckel (1981); Torres (1987) and Boggs & Bohm-Vitense (1989). The stars No. 68 (B0V) and LSS 4627 (B1V) have been classified for the first time. The former exhibits a narrow emission in the $H\beta$ core that could be attained to a nebular contribution. We find that star No. 9 has an anomalous color excess for its spectral type. We observed a SBD in the spectra of the Nos. 45 and 65. This confirms that the star No. 65 is a Be star which is shown in Fig. 13. Instead, we found that star No. 45 is a supergiant. According to the location of the stars Nos. 73 and 93 in the HR diagram, they cannot be classified as blue stragglers.

5. The population of B, Be and Bdd stars

We used the BCD method to derive physical properties of a large number of stars (~ 230) in the direction of the open clusters Collinder 223, Hogg 16, NGC 2645, NGC 3114, NGC 3766, NGC 4755, NGC 6025, NGC 6087, NGC 6250, NGC 6383 and NGC 6530 (see Paper I, Paper II and this work). Thus, we gathered a homogeneous set of fundamental parameters that in addition are not affected by the interstellar/circumstellar reddening. This way we were able to obtain cluster parameters of 11 open clusters, construct well-defined HR diagrams and perform a better identification of the cluster star members. At the same time, the study of the BD enables the detection of circumstellar envelopes around B-type stars in an independent way of the typical criterion based on the presence of emission H lines. This is possible through the observation of a SBD.

In this section, we discuss the derived BCD stellar fundamental parameters and describe the main characteristics of the population of B stars. Particularly, we present global properties of stars with circumstellar envelopes.

5.1. The BCD stellar fundamental parameters

The discussion of the fundamental parameters is based on a reduced sample of 198 early-type stars, classified as members (*m*) and probable members (*pm*), of the 11 open clusters studied. We discarded *pnm* or *nm* stars from this analysis.

Firstly, we compare the BCD fundamental parameters of all the stars, T_{eff} and M_v , with the scarce values reported in the literature. This comparison is shown in Fig. 9 where we

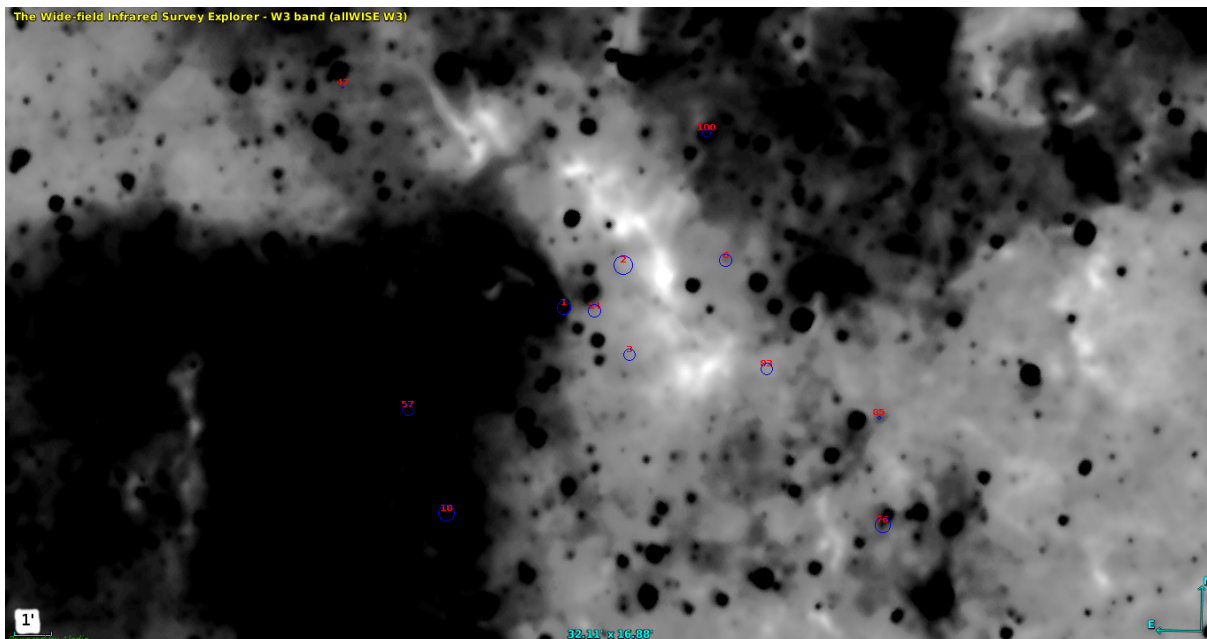


Fig. 5. Idem Fig. 1 but for NGC 6383.

Table 5. NGC 6383: Previous and current determinations of color excess, distance, and age.

Reference	$E(B - V)$ [mag]	$(m_v - M_v)_0$ [mag]	d [pc]	age [Myr]
Trumpler (1930) ^{sp}	2130	...
Zug (1937) ^{ph}	2130	...
Sanford (1949) ^{sp}	760	...
Eggen (1961) ^{ph}	1259	...
Graham (1967) ^{ph}	...	10.68 ± 0.54	1380	...
Lindoff (1968) ^{ph}	...	10.5	1250	~ 20
Becker & Fenkart (1971) ^c	0.26	10.92	1065	...
Fitzgerald et al. (1978) ^{ph,sp}	0.33 ± 0.02	10.85	1500 ± 200	1.6 ± 0.4
Lloyd Evans (1978) ^{ph}	0.35	10.6	1350	...
The et al. (1985) ^{ph}	0.30 ± 0.01	...	1400 ± 150	...
Pandey et al. (1989) ^{ph}	0.35	11.65	...	~ 4
Battinelli & Capuzzo-Dolcetta (1991) ^{sp}	1380	~ 4
Feinstein (1994) ^{ph}	0.33	...	1400	...
Rastorguev et al. (1999) ^h	1180	...
Kharchenko et al. (2005) ^h	985	~ 5
Paunzen et al. (2007) ^{ph}	0.28 ^{**}	...	1700	4
Piskunov et al. (2008) ^h	0.30	10.897
Rauw & De Becker (2008) ^{ph}	0.32 ± 0.02	...	1300 ± 100	...
This work	0.51 ± 0.03	9.61 ± 0.38	834 ± 158	$\sim 3 - 10$

Notes. ^(c) Results based on catalog data. ^(h) Results based on HIPPARCOS data. ^(ph) Results based on photometric data. ^(sp) Results based on spectroscopic data. ^(**) The color excess $E(B - V)$ was calculated in this work, using the published $E(b - y)$ value and the relation $E(b - y) = 0.74 E(B - V)$.

distinguish normal B-type stars (identified with circles) from those that have circumstellar envelopes (identified with triangles). The effective temperatures were taken from McSwain et al. (2008, 2009, NGC 3766), Dufton et al. (2006, NGC 4755), Piskunov (1980, NGC 6025), and van den Ancker et al. (2000, NGC 6383). Whilst the absolute visual magnitudes were gathered from Clariá & Lapasset (1991, Collinder 223), Fitzgerald et al. (1979b, Hogg 16), Fitzgerald et al. (1979a, NGC 2645),

Shobbrook (1985, NGC 3766), Kilambi (1975, NGC 6025) and Lloyd Evans (1978, NGC 6383)⁴.

In relation to the BCD T_{eff} values (see Fig. 9a), we note that in general they are systematically greater than those derived by other techniques. It has been shown that the effective temperatures derived with the BCD method have no significant differences with the values derived from multicolor photometric systems, line-blanketed models and the infrared flux method (Cidale

⁴ We only consider works that explicitly published M_v values for individual stars.

Table 6. NGC 6530: Previous and current determinations of color excess, distance, and age.

Reference	$E(B - V)$ [mag]	$(m_v - M_v)_0$ [mag]	d [pc]	age [Myr]
Trumpler (1930) ^{ph}	1 090	...
Sanford (1949) ^{sp}	730	...
Johnson et al. (1961) ^{ph}	0.32	10.7 ± 0.3	1 400	...
Penston (1964) ^p	~ 1
Lindoff (1968) ^{sc}	...	11.91	1 560	< 7
van Altena (1972) ^{ph}	0.35	11.25	1 780	2
Harris (1976) ^{sp}	6.36 ± 0.34
Kilambi (1977) ^{ph}	0.34	10.7
Sagar & Joshi (1978) ^{ph}	0.35	11.3	...	2
Chini & Neckel (1981) ^{ph,sp}	0.36 ± 0.09	11.4
Boehm-Vitense et al. (1984) ^{sp}	5 ± 2
Sagar et al. (1986) ^{ph}	~ 2
Battinelli & Capuzzo-Dolcetta (1991) ^p	0.35	...	1 600	~ 2
Strobel et al. (1992) ^p	0.4	12.7	...	~ 3
Feinstein (1994) ^{ph}	0.36	11.4	1 900	...
van den Ancker et al. (1997) ^{ph,sp}	0.30	...	$1\,800 \pm 200$...
Rastorguev et al. (1999) ^h	1 270	...
Robichon et al. (1999) ^h	~ 763.36	...
Sung et al. (2000) ^{ph}	0.35	11.25 ± 0.1	...	1.5
Baumgardt et al. (2000) ^h	~ 917.43	...
Loktin & Beshenov (2001) ^h	...	9.005 ± 0.255	...	~ 7.5
Prisinzano et al. (2005) ^{ph}	1 250	2.3
Kharchenko et al. (2005) ^h	1 322	~ 4.7
McSwain & Gies (2005) ^{ph}	0.34^{**}	10.62	...	~ 7.4
Zhao et al. (2006) ^{ph}	1 330	~ 7.4
Mayne & Naylor (2008) ^p	0.32	10.34	...	2
Kharchenko et al. (2009) ^h	0.30	...	1 322	~ 4.7
Kharchenko et al. (2013) ^h	0.541	...	1 365	~ 4.7
This work	0.26 ± 0.05	11.76 ± 0.20	$2\,245 \pm 215$	4 – 6

Notes. ^(h) Results based on HIPPARCOS data. ^(p) Results based on published data. ^(ph) Results based on photometric data. ^(sc) Results based on synthetic clusters. ^(sp) Results based on spectroscopic data. ^(**) The color excess $E(B - V)$ was calculated in this work, using the published $E(b - y)$ value and the relation $E(b - y) = 0.74 E(B - V)$.

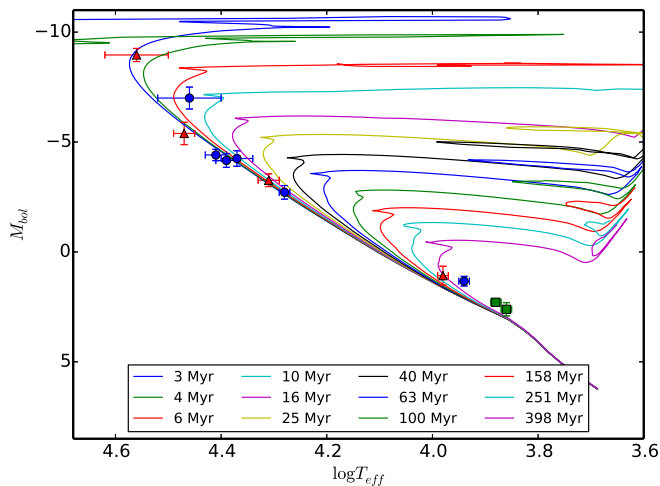


Fig. 6. NGC 6383: HR diagram. The estimated age for this cluster is between 3 and 10 Myr. The isochrone curves are given by Ekström et al. (2012). Members and probable members of the clusters are denoted in ● (blue) symbols and probable non-members and non-members in ■ (green). Star members with circumstellar envelopes are indicated in ▲ (red).

et al. 2007). Therefore, we observe that our T_{eff} determinations show discrepancies of about $\Delta T_{\text{eff}} \lesssim 2000$ K, with those obtained by McSwain et al. (2008, 2009, $H\alpha$ and Strömgren photometry) and Dufton et al. (2006, non-LTE atmospheric models). Instead, significant discrepancies are observed in some of the stars of NGC 6025. On the other hand, we have three stars in common with van den Ancker et al. (2000) and only the star NGC 6383 6 shows a huge discrepancy. Perhaps, this could be due to the too late spectral classification assigned to this star by these authors.

Regarding the M_v values, we have to consider that in most of the cases these were calculated using the distance modulus of the cluster. Therefore, we can only compare values obtained for stars belonging to clusters that have similar $(m_v - M_v)_0$ as ours. Such clusters are Collinder 223, NGC 3766, NGC 6025 and NGC 6383. This comparison is shown in Fig. 9b. The greatest discrepancies, this means values with $|M_{\text{VBCD}} - M_{\text{Viii}}| > 2$ mag, are found among stars reported as Em, Be, supergiant or variable⁵. It worth mentioning that most of the cited works consider average

⁵ These stars are: Cr 223 35 (reported as blue straggler), Hogg 16 2 (reported as Em), Hogg 16 3 (reported as Em), Hogg 16 9 (reported as Em), NGC 2645 1 (classified as supergiant), NGC 2645 2 (classified as supergiant), NGC 3766 15 (reported as Be), NGC 3766 232 (reported as vari-

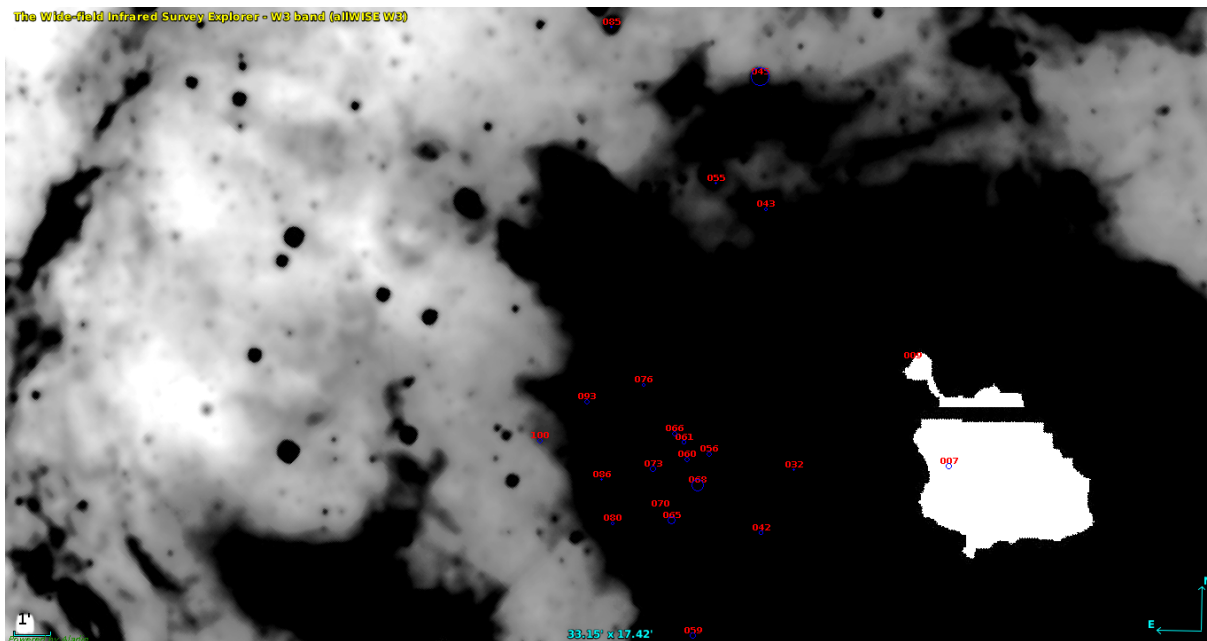


Fig. 7. Idem Fig. 1 but for NGC 6530. The image is saturated (white patch).

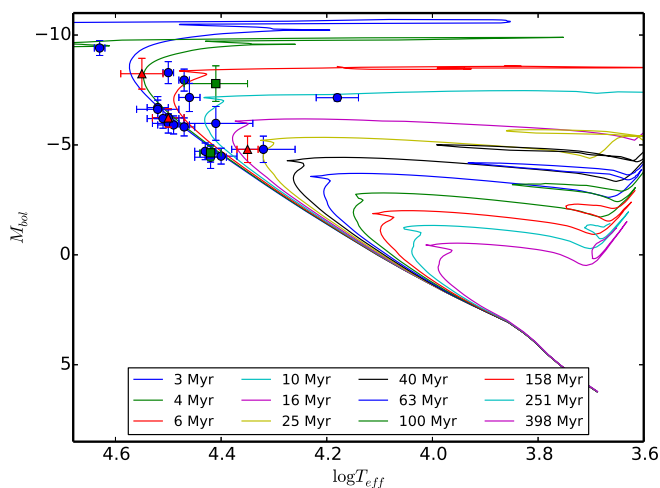


Fig. 8. NGC 6530: HR diagram. The estimated age for this cluster is 4 – 6 Myr. The isochrone curves are given by Ekström et al. (2012). Members and probable members of the clusters are denoted in • (blue) symbols and probable non-members and non-members in ■ (green). Star members with circumstellar envelopes are indicated in ▲ (red).

values of $E(B - V)$ and these could lead to the discrepancies observed in stars with circumstellar envelopes.

In relation with comparisons of absolute bolometric magnitudes and surface gravities (see Fig. 10) derived from stellar evolution models with the BCD parameters, we can behold that both show the same trends found in Paper I. In that opportunity only the results for NGC 3766 and NGC 4755 were considered. We highlight the excellent agreement between BCD and evolutive M_{bol} values as is depicted in Fig. 10a. Whilst the discrepant behavior in $\log g$ (see Fig. 10b) was already mentioned in Paper I and it is related to the technique used to derive the surface gravity. The $\log g$ values derived from the BCD method

able), NGC 3766 291 (reported as Be), NGC 6383 6 (reported with an IR excess), and NGC 6383 47 (classified as a bright giant)

($\log g(\lambda_1, D)$) are also called atmospheric gravities, since the BCD calibration of this quantity is based on parameters $\log g$ determined by fitting observed $H\gamma$ and $H\beta$ line profiles with synthetic ones, obtained with classical model atmospheres. On the contrary, $\log g_{\text{evol}}$ are calculated using bolometric magnitudes $M_{\text{bol}}(\lambda_1, D)$ and effective $T_{\text{eff}}(\lambda_1, D)$ read on the BCD calibrations, which produce estimates of the stellar radius R/R_{\odot} , while they lead to masses M/M_{\odot} read on the stellar evolutionary tracks. For stars with $M \lesssim 12 M_{\odot}$ and radii $R \lesssim 12 R_{\odot}$, the value of $\log g_{\text{evol}}$ is often estimated in the deep stellar layers while $\log g_{\text{atm}}$ is more related to the outermost atmospheric layers. A reverse situation would occur for evolved massive stars with $M \gtrsim 20 M_{\odot}$ and $R \gtrsim 40 R_{\odot}$.

The observed deviation between the $\log g_{\text{evol}}$ and $\log g(\lambda_1, D)$, mostly at $\log g \lesssim 3.7$ has already been noted by Gerbaldi & Zorec (1993) for late B- and early A-type stars. This deviation is due to an overestimate of the stellar mass possibly carried by difficulties on the stellar structure calculations at the helium ionization region (Maeder, private communication).

It is worth noting that rotation, whose effects are neglected in the present analysis, would act with systematic differences in the $\log g$ determinations that range in the opposite way as noted above for stars with $M \lesssim 12 M_{\odot}$. The $\log g$ corrected for rapid rotation effect, called pnr (parent non-rotating counterpart) surface gravities (Frémat et al. 2005), are generally larger by about 0.14 ± 0.14 dex than the observed or apparent ones. However, differences are largely aspect-angle dependent (Zorec et al. 2016).

Therefore, we should find higher apparent bolometric luminosities and lower effective temperatures than those expected for non-rotating stellar counterparts (Frémat et al. 2005; Zorec et al. 2005). As a consequence we will have lower $\log g_{\text{evol}}$ determinations than the values for non-rotating cases.

5.2. Comments on the Balmer discontinuity of Be stars

The photospheric component of the BD is determined by the flux ratio $D_* = \log(F_{3700}^+/F_{3700}^-)$. F_{3700}^+ is given by the interception of the extrapolated straight line “A” that fits the Paschen continuum,

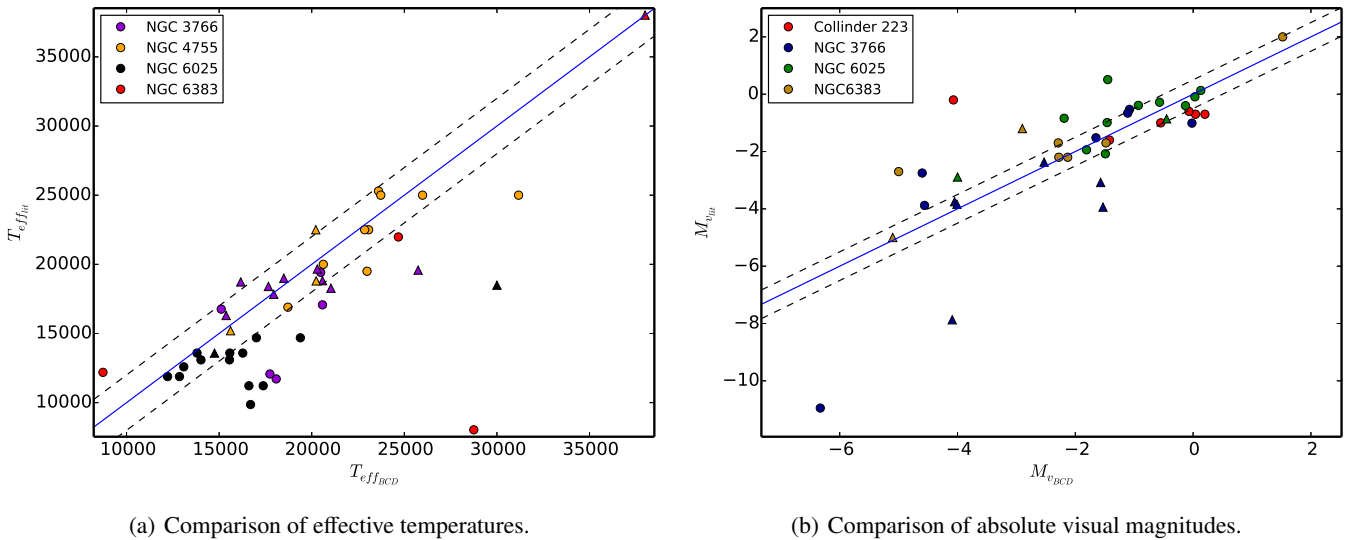


Fig. 9. Comparison of BCD T_{eff} and M_v values determined for member stars with those determined in previous works. The straight line is the identity function and the dotted lines deviate from it in 2000 K and 0.5 mag, respectively. Circle symbols identify normal B-type stars and triangles are used for stars with circumstellar envelopes.

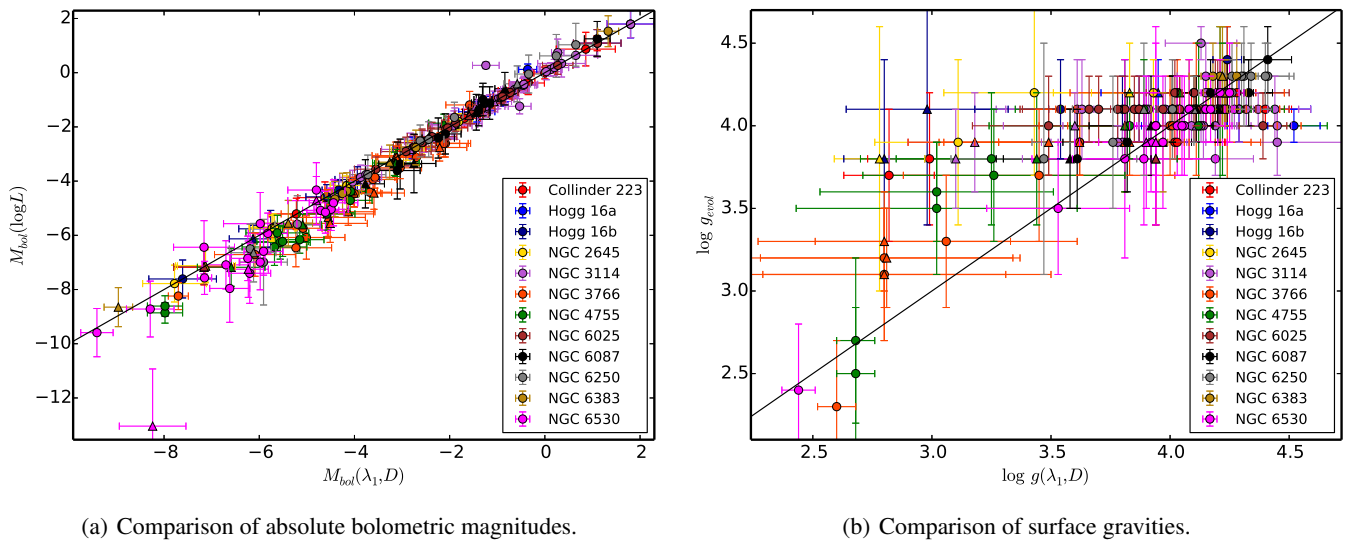


Fig. 10. Comparison of $M_{\text{bol,evol}}$ and $\log g_{\text{evol}}$ parameters, derived from stellar evolution models, against BCD $M_{\text{bol}}(\lambda_1, D)$ and $\log g(\lambda_1, D)$ estimates. Circles identify normal B-type stars and triangles stars with circumstellar envelopes. The straight line corresponds to the identity function.

shown in Fig. 11, and a vertical line at $\lambda = 3700 \text{ \AA}$ and F_{3700}^- is given by the interception of same vertical line and the envelope curve “B” that passes over the absorption cores of the higher members of the Balmer lines until the point they merged.

Let us recall some characteristics of these fluxes:

1) F_{3700}^+ represents the flux density that would exist if the wings of the higher members of the Balmer lines series (H_n ; $n > 8$) do not overlap. This line overlapping produces a pseudo-continuum (represented by the last Balmer lines merged at redward the upper curve “C” surrounding the Balmer lines in Fig. 11). Due to this overlapping and the low resolution of the spectra, the last Balmer lines merged redwards to the theoretical value, $\lambda \sim 3648 \text{ \AA}$.

2) This pseudo-continuum intercepts also the Balmer continuum shortly after the BD in O-, B-, A-, F-type stars without circumstellar emission or absorption.

3) F_{3700}^- also belongs to the above mentioned pseudo-continuum, and as both fluxes F_{3700}^\pm are measured at the same wavelength they are affected by nearly the same amount of emission or absorption, ΔF_{3700} , originated by a circumstellar envelope. For this reason, Papers I and II of this series explain our care in determining where the last lines of the Balmer series overlap. The circumstellar emission or absorption have very little if any incidence on the determination of the photospheric BD, D_* . Therefore, the BD of some stars with circumstellar envelopes can be defined as the quantity $D = D_* + d$, where D_* is the height of the photospheric (or first) component of the BD and d represents the height of the SBD. The first component of the BD (D_*) has always been observed constant in Be stars, within the limits of uncertainties of the BCD system (0.015 dex in D and $1 - 2 \text{ \AA}$ in λ_1 , De Loore et al. 1979; Divan et al. 1983; Divan & Zorec 1982; Zorec 1986; Zorec et al. 1989; Zorec & Briot 1991; Vinicius et al. 2006; Cochetti et al. 2013, 2015). Apart from the

rare case of γ Cas (O9Ve, HD 5394) in 1935 and 1938 (Barbier & Chalonge 1939), the constancy of D_* has even been noted in stars with $\text{Be} \rightleftharpoons \text{B} \rightleftharpoons \text{Be}$ -shell-phase changes such as: γ Cas, Pleione, 88 Her and 59 Cyg.

However, as D_* is determined empirically it does not avoid two effects caused by the presence of a circumstellar envelope, which nonetheless are very small:

a) The genuine photospheric fluxes F_{3700}^\pm transform into $F_{3700}^\pm + \Delta F_{3700}$, so that:

$$D_*^{\text{obs}} \simeq D_*^o + \left(\frac{\Delta F_{3700}}{F_{3700}^+} \right) (1 - 10^{D_*^o}), \quad (1)$$

where D_*^o represents the actual photospheric BD, which in the hottest stars is

$$\Delta F_{3700}/F_{3700}^+ \lesssim 0.05 \quad (2)$$

b) On the other hand, since F_{3700}^+ is obtained by extrapolation, it is affected by the color effects in the Paschen continuum carried by the λ^3 dependency of the circumstellar envelope opacity. Moujtahid et al. (1998, 1999) and Gkouvelis et al. (2016) estimated these effects and obtained that

$$D_* = D_*^{\text{obs}} + \epsilon_D$$

with (3)

$$\epsilon_D \simeq 0.02 \times [\Phi^{\text{obs}} - \Phi(\lambda_1, D_*^o)],$$

Note that as the compilation made by Moujtahid et al. (1998) actually corresponds to spotted measurements concerning otherwise long-term Be-star "bumper" activity (Cook et al. 1995; Hubert & Floquet 1998; Hubert et al. 2000; Keller et al. 2002; Mennickent et al. 2002; de Wit et al. 2006) the color changes are of the order of $\Phi^{\text{obs}} - \Phi(\lambda_1, D_*^o) \lesssim 0.5 \mu\text{m}$ and the error committed by this effect on the estimate of the photospheric BD is $\epsilon_D \lesssim 0.010$ dex. This error carries uncertainties on the estimate of the visual absolute magnitude which is smaller than the deviations of the absolute magnitude within a spectral type-luminosity class curvilinear box of the BCD system (Chalonge & Divan 1973; Zorec et al. 2009).

The SBD is caused by the flux excess produced in the circumstellar envelope due to bound-free and free-free transitions, mostly of hydrogen and helium atoms and electron scattering. Therefore, as spectrophotometric variations of Be stars are currently different according to the Be phases, emission phases, i.e. $d < 0$ are generally accompanied by a brightening and a reddening of the Paschen continuum, while shell phases ($d > 0$) generally show a little decrease of the stellar brightening, but without changing the color of the Paschen continuum. An extensive compilation of these spectrophotometric behaviors was published by Moujtahid et al. (1998).

The height of the SBD, d , is then measured as the flux difference (in a logarithmic scale) between the observed Balmer continuum fitted by a straight-line "E" and a parallel line "F" to Balmer continuum through the point defined by the merged of the Balmer lines provides a measurement of d (see Fig. 11).

5.3. Stars with circumstellar envelopes

During the process of seeking emission line stars in the direction of the 11 studied open clusters we found a total of 46 Be

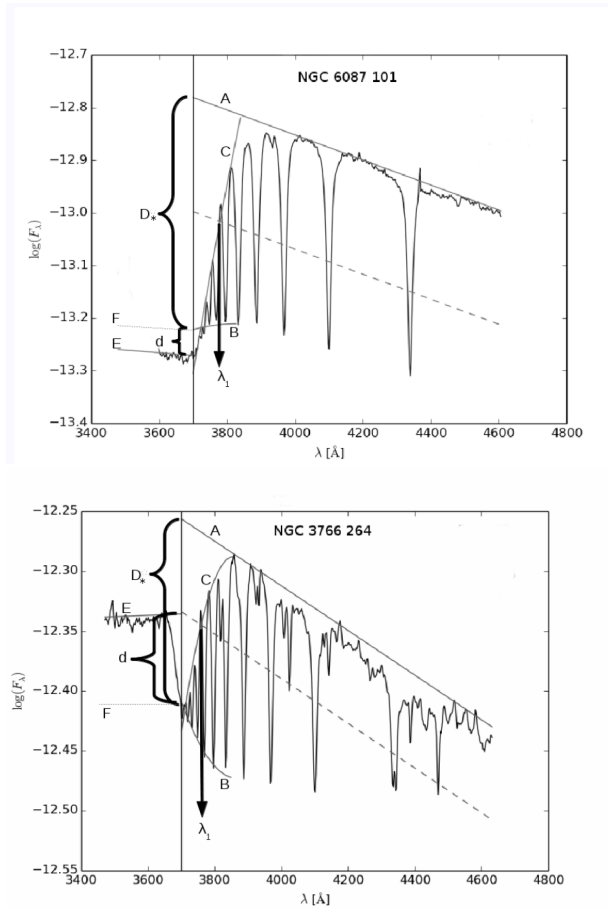


Fig. 11. Stars with a second Balmer discontinuity. D_* is the height of the photospheric component of the Balmer discontinuity and d is the height of the second component. In the upper panel d is in absorption (Be-shell phase) and in the lower panel is in emission (Be phase).

stars (6 new Be stars: Cr 223 2, NGC 2645 5, NGC 3766 301, HD 308 852, NGC 6087 7, and NGC 6383 76)⁶ when considering the whole sample of 230 stars. Among these 46 Be stars we detected 19 objects with a SBD.

In addition, we found 15 B-type stars with a SBD that show neither line emission features nor have been previously reported as Be stars, and 3 B supergiants (BSG) with a SBD (HD 74 180, NGC 4755 1, NGC 6530 45). The 15 B-type stars that show a SBD could be Be candidates, these stars will be called hereafter Bdd (B stars with a double Balmer discontinuity). In this way, the total number of stars with a SBD (Bdd+Be+BSG stars) is 37, which were identified in the corresponding tables of Papers I, II and this work, with a supra index dd (stars NGC 3766 55 and NGC 3114 126 were discarded since they have a doubtful SBD). Therefore, our whole sample of objects with a SBD in absorption consists of 29 stars (3 in Cr 223, 1 in Hogg16a, 2 in NGC 2645, 10 in NGC 3114, 1 in NGC 3776, 1 in NGC 4755, 2 in NGC 6025, 7 in NGC 6087, 1 in NGC 6383, and 1 in NGC 6530) and 8 in emission (2 in Cr 223, 1 in Hogg16b, 2 in NGC 3776, 1 in NGC 4755, 1 in NGC 6250, 1 in NGC 6530).

Henceforth we will restrict ourselves to study the sample of Be and Bdd stars belonging to the 11 studied galactic clusters. This sample includes 42 Be (17 with a SBD) and 13 Bdd stars, mainly of B-type stars, although a few late O and early A stars were also observed. Among the 42 Be stars we found 30

⁶ We observe $H\alpha$ in emission in the spectrum of these stars.

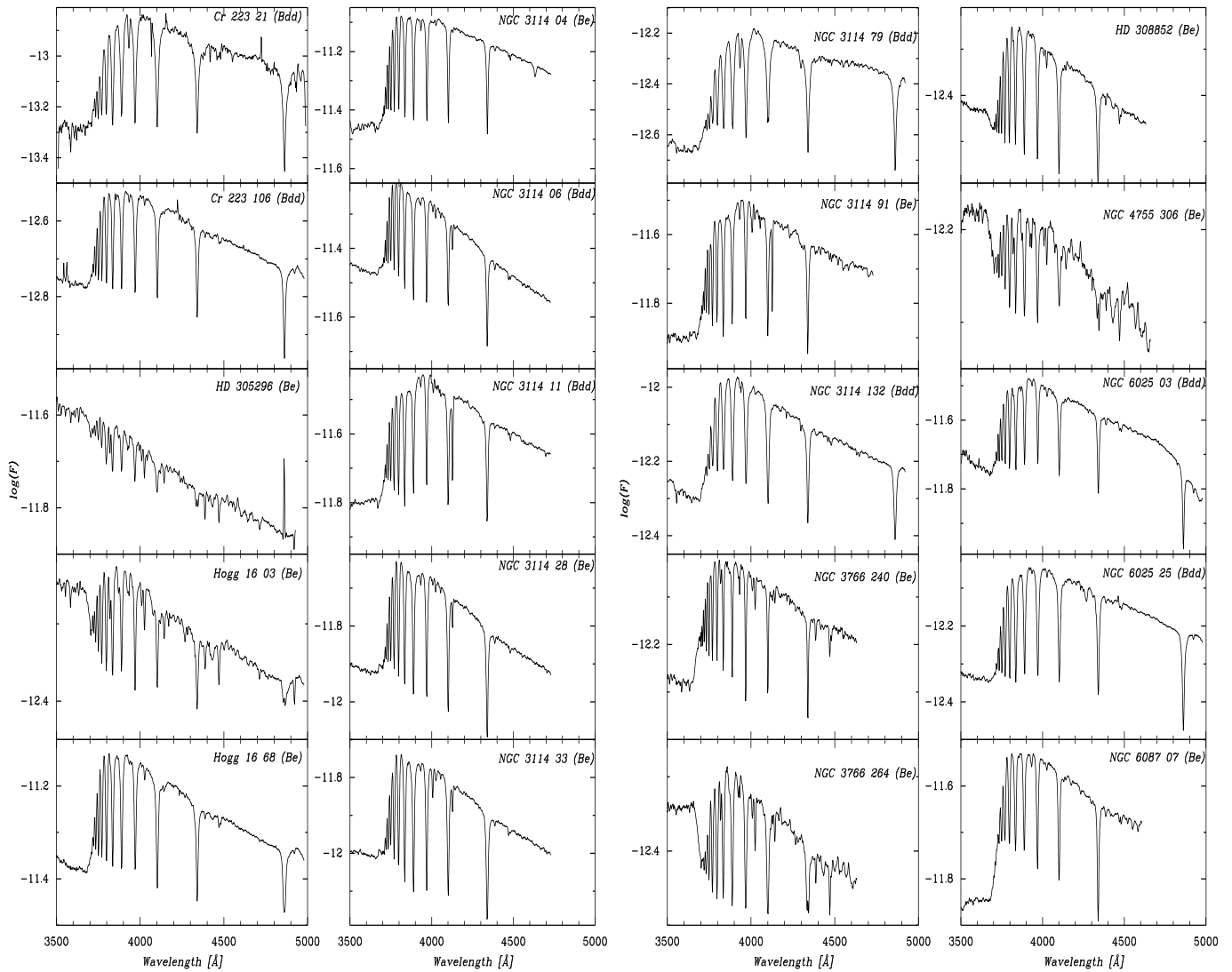


Fig. 12. Low resolution spectra of stars with a SBD.

dwarfs (e.g. luminosity classes IV, V and VI) and 12 slightly more evolved stars (e.g. luminosity classes III and II). Thus, considering only the sample actually observed in the BCD system, which encompass $N_{\text{tot}} = 198$ B+Be+Bdd stars (luminosity classes from ZAMS to bright giants) of which $N_e = 42$ are Be stars, we obtain $f = N_e/N_{\text{tot}} = 21\%$. This percentage is higher than that reported by Zorec & Briot (1997) for the field of galactic Be stars ($\sim 17\%$). While among the 13 ($\sim 7\%$), 11 are dwarfs and 2 are giants. Table 7 lists the Be and Bdd stars used for this analysis.

We notice that according to the weather conditions, several observing restrictions and other stellar sample selections, the above fraction $f = 21\%$ of B emission-line stars can be biased, mainly because part of the sample of Be stars were not selected randomly. In order to evaluate a possible overestimate of the actual fraction of Be stars that we have calculated for open clusters, we first compare this fraction with the fraction that can be derived using the available Be and B stars in the WEBDA database for the same 11 clusters. Thus, in the WEBDA database we counted 57 Be stars among 236 B stars. This implies a fraction of 24% which is larger than the one we have estimated in

this work. However, we must keep in mind that not all stars in the WEBDA database are necessarily cluster members.

A second test is to compute a Monte Carlo simulation of the distribution of an "actual" fraction, $f_{\text{actual}} = 21\%$ B emission-line stars for $N_{\text{tot}} = 198$ B+Be+Bdd stars in 11 open clusters, over 100 independent samplings. We obtained thus an average $\langle f_{\text{simulated}} \rangle = 22\%$ B emission-line stars with dispersion $\sigma_f = 9\%$. If we had observed $N_{\text{tot}} = 2000$ B+Be+Bdd stars, the simulation predicts that we should have $\langle f_{\text{simulated}} \rangle = 22\%$ B emission-line stars with $\sigma_f = 4\%$. In this simulation we have assumed that all clusters have the same age, so that each can be able to bear the same fraction of B emission-line stars. Considering differences in cluster ages, the bias σ_f could perhaps be larger.

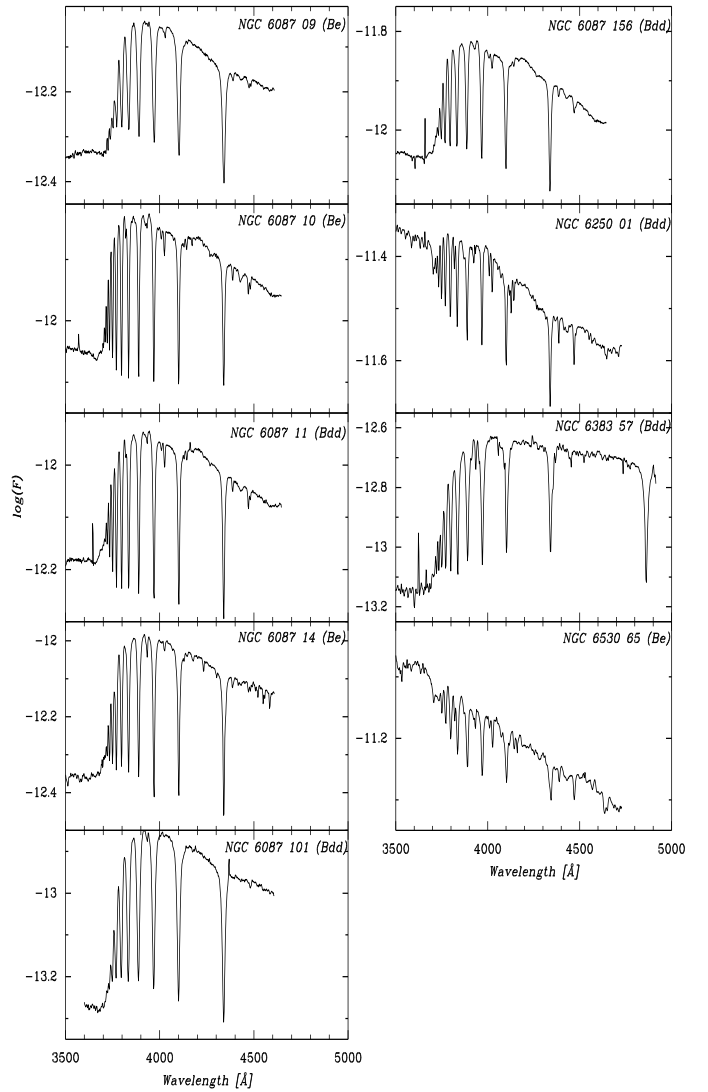
Hence, both results suggest that the fraction of Be stars in open clusters is probably larger than that of field Be stars.

The spectra of these 13 Bdd stars are shown in Figs. 12 and 13 together with the spectra of the 17 Be stars with a SBD. Moreover, we have high resolution spectra of only 7 Bdd stars in the region of $H\alpha$. With the exception of NGC 3114 11 that show a typical shell profile, the rest of the stars display an absorption $H\alpha$ line (see Fig. 14) that might be partially filled in by emis-

Table 7. Be and Bdd stars belonging to open clusters.

ID	ST	Group	Paper Reference
Cr 223 021 ^{dd}	A1V	Bdd	II
Cr 223 106 ^{dd}	B5IV	Bdd	II
HD 305 296 ^{dd}	B0Ve	Be	II
Hogg 16a 68 ^{dd}	B4Ve	Be	II
Hogg 16b 02	B2II	Be	II
Hogg 16b 03 ^{dd}	B1IIIe	Be	II
NGC 2645 03	B0II	Be	II
NGC 2645 04	B0IIe	Be	II
NGC 2645 05	B1IVe	Be	II
NGC 3114 003 ^{dd}	B6IIIe	Be	II
NGC 3114 004 ^{dd}	B8IIIe	Be	II
NGC 3114 006 ^{dd}	B8IV	Bdd	II
NGC 3114 011 ^{dd}	B8IV	Bdd	II
NGC 3114 028 ^{dd}	B6IVe	Be	II
NGC 3114 033 ^{dd}	B5IVe	Be	II
NGC 3114 079 ^{dd}	A1V	Bdd	II
NGC 3114 091 ^{dd}	B8IVe	Be	II
NGC 3114 129	B8Ve	Be	II
NGC 3114 132 ^{dd}	B7:VI:	Bdd	II
NGC 3766 001	B5III	Be	I
NGC 3766 015	B4III	Be	I
NGC 3766 026	B2IVe	Be	I
NGC 3766 027	B3III	Be	I
NGC 3766 151	B3Ve	Be	I
NGC 3766 239	B3IV	Be	I
NGC 3766 240 ^{dd}	B5IIe	Be	I
NGC 3766 264 ^{dd}	B2Ve	Be	I
NGC 3766 291	B3Ve	Be	I
NGC 3766 301	B3Ve	Be	I
HD 308 852 ^{dd}	B5IVe	Be	I
NGC 4755 008	B3V	Be	I
NGC 4755 011	B6V	Be	I
NGC 4755 117	B3V	Be	I
NGC 4755 202	B2IV	Be	I
NGC 4755 306 ^{dd}	B0IIIe	Be	I
NGC 6025 01	B0Ve:	Be	II
NGC 6025 03 ^{dd}	B5III	Bdd	II
NGC 6025 06	B6V	Be	II
NGC 6025 25 ^{dd}	B7V	Bdd	II
NGC 6087 007 ^{dd}	B6Ve	Be	III
NGC 6087 009 ^{dd}	B6Ve	Be	III
NGC 6087 010 ^{dd}	B5IIIe	Be	III
NGC 6087 011 ^{dd}	B4V	Bdd	III
NGC 6087 014 ^{dd}	B8V	Be	III
NGC 6087 022	B2IVe	Be	III
NGC 6087 101 ^{dd}	A1:VI:	Bdd	III
NGC 6087 156 ^{dd}	B6:V:	Bdd	III
NGC 6250 01 ^{dd}	B0III	Bdd	III
NGC 6250 35	B0IVe	Be	III
NGC 6383 001	O7V	Be	III
NGC 6383 057 ^{dd}	A2V	Bdd	III
NGC 6383 076	B3Ve	Be	III
NGC 6530 042	B0IV	Be	III
NGC 6530 065 ^{dd}	O	Be	III
NGC 6530 100	B2VI	Be	III

Notes. ^(dd) Star with a SBD.


Fig. 13. Idem Fig. 12.

sion. However, as these spectra were not taken simultaneously with the spectrophotometric BCD observations either emission or shell features, if they existed, could have disappeared in the meantime.

5.4. The T_{eff} -log g diagram

In Fig. 15 we present a T_{eff} -log g diagram derived with the BCD parameters, where we can observe that most of the B and Be stars are dwarfs ($3.5 \leq \log g \leq 4.5$) and are distributed in the whole temperature interval. A smaller number of B and Be giants seem also to be uniform distributed in the same T_{eff} range. This supports the results found by Mermilliod (1982); Slettebak (1985); Zorec et al. (2005) who state that Be stars occupy the whole main sequence band and the Be phenomenon occurs in very different evolutionary states. On the other hand, the sample of Bdd stars is mainly constituted by cool B dwarfs with circumstellar envelopes, as shown in next section.

5.5. Distribution of stars per spectral subtype and age

It has to be emphasized that our sampling is far from being complete due to the observing conditions (short running campaigns or full moon nights) that introduced strong selection effects, since sometimes we only could observe the brightest members of each clusters. However, we took care of observing almost all previously reported Be stars. Notwithstanding of the small sample size and risk of bias in the included trials, it is still possible to discuss age-dependence trends related to the appearance of the Be phenomenon, as was previously suggested by Mathew et al. (2008); Zorec et al. (2005); Fabregat & Torrejón (2000), and compare these trends with the presence of the new group of Bdd stars. To this purpose we classified our sample in three age groups. The first group comprises open clusters with ages between 3 Myr and 10 Myr, the second one is related with intermediate-age clusters (10 – 40 Myr) and the last group encompasses clusters older than 40 Myr.

For each age group we calculated the relative frequency of different kinds of stars: B, Be and Bdd, per interval of spectral subtype. To avoid skewing the results we searched for optimal bin number and bin size per spectral subtype. Hence, we adopted a bin-width optimization method that minimized the integrated squared error (Shimazaki & Shinomoto 2007). We obtained a total of 6 bins that correspond to the spectral intervals: B0-B2, B2-B4, B4-B6, B6-B8, B8-A0, and A0-A2. The corresponding bar-graph histograms per spectral subtype and per age group are illustrated in Fig. 16, where the blue, red and green bars represent, respectively, the relative frequency of normal B, Be and Bdd stars within each bin.

In the plots we observe that young and intermediate-age clusters are composed of Be stars of mostly B2-B4 spectral types and only a few Bdd stars were detected (Fig. 16a and b). We have a fraction of about 19% of Be stars in young open clusters (< 10 Myr). This number then enhances to about a 28% for the intermediate-age group (with ages between 10 – 40 Myr, see Fig. 16b) where we have the maximum Be star fraction, supporting thus previous results found by Malchenko (2008) and Fabregat & Torrejón (2000). In the intermediate-age group we found also a great number of evolved Be stars with luminosity III-II. Furthermore, in the same plot, we can observe a small fraction of Be stars at the B4-B6 types. Then, the percentage of Be stars seems to decrease in the old open clusters (~ 17%, Fig. 16c), as was stressed by Mermilliod (1982) and Grebel (1997). In these old clusters, the Be phenomenon is dominated by stars with spectral types later than B4 and the maximum frequency of Be stars is around the B6-B8 types. This result indicates a clear trend of the appearance of the Be phenomenon with age.

On the other hand, if we focus on the relative frequency of Bdd stars (stars with circumstellar envelopes that are out off an emission phase) per spectral subtype (Fig. 16c), a significant number (~ 12%) of Bdd stars later than B5 is present and its distribution seems to follow the frequency distribution of B and “active” Be stars. Therefore, the distribution of Bdd stars seems to complete, in number, the lack of late “active” Be stars. We interpret the result in the same sense as Zorec et al. (2003)’s hypothesis which states that the strong deficiency of the field Be stars cooler than B7 perhaps could be taken on by Bn stars (i.e., B stars with broad absorption lines). Zorec et al. (2003) also proposed that the absence of late Be stars and the increment of Bn stars is mainly due to the fact that their low effective temperatures are not able to keep their circumstellar envelopes completely ionized. Thus, Bn stars could be latent Be and Be-shell stars (Zorec et al. 2003; Ghosh et al. 1999). Therefore, it would

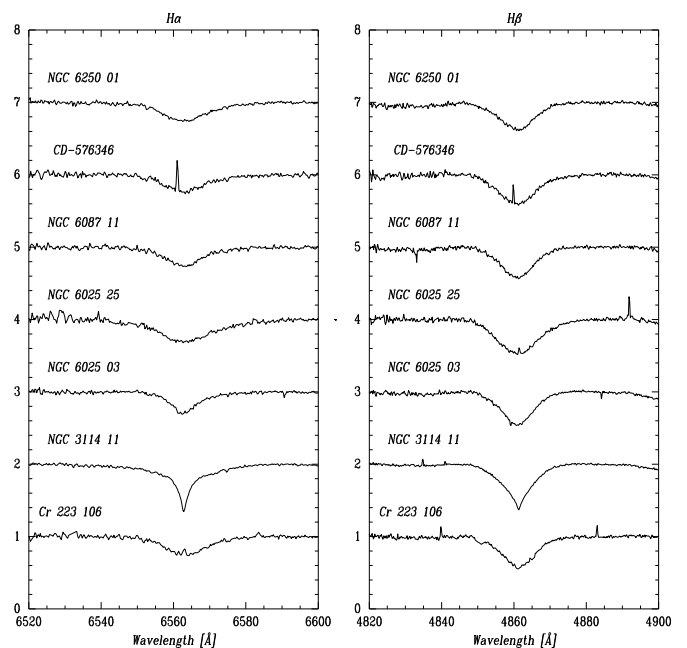


Fig. 14. Bdd H α (first column) and H β (second column) profile lines.

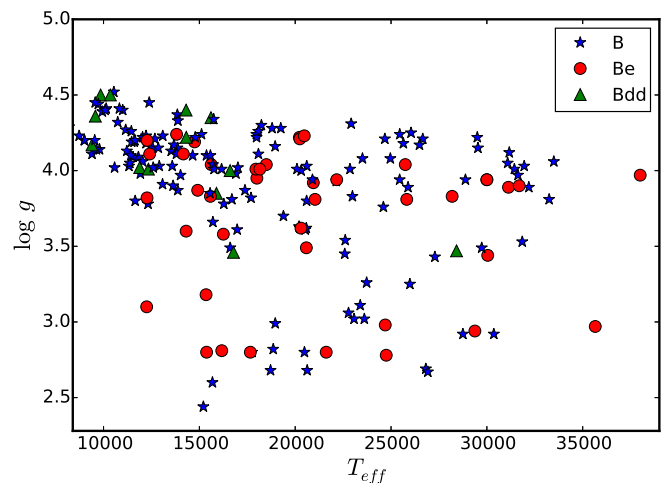


Fig. 15. Cluster star members in T_{eff} against $\log g$ plot. Be stars are distributed in the whole temperature interval.

be necessary to study in more detail the properties of the Bn star population and a possible link with the Bdd star group, if they are not the same population.

In summary, the Be phenomenon is observed in both dwarf and giant stars along the whole main sequence. In addition we confirm the trend of an age evolution of the Be phenomenon, since among the massive stars the Be phenomenon seems to appear on average at an earlier age than in the less massive stars. This result confirms previous age-dependence trends found by Mathew et al. (2008); Zorec et al. (2005); Fabregat & Torrejón (2000). In addition, we found that the number of stars with circumstellar envelopes (active and passive B emission stars) in the old age cluster group amounts to 29%, suggesting that Bdd stars might be the coldest counterpart of stars with the Be phenomenon.

From a theoretical point of view, the age evolution of the Be phenomenon was supported by Ekström et al. (2008). These authors showed that the age-dependence of the Be phenomenon could be related to the increase of the ratio $V \sin i/V_{\text{crit}}$ due to a lowering of V_{crit} (critical rotation velocity) of stars with age, via the transport of angular momentum by meridional circulation to the star's surface and stellar wind. On the other hand, the rotation modifies stellar pulsations, since centrifugal force distorts the resonant cavity of the pulsations and the Coriolis force modifies the modes' dynamic (Ouazzani et al. 2012). As well, the evolutionary changes affect the pulsational properties of the stars due to changes in the gravity, as well as the isentropic sound velocity and density (Bruggen & Smeyers 1987). Therefore, both rotation and pulsation modes might compete to release material from the star to fill a disk. Therefore, our knowledge about the evolution effects of rotation and pulsational modes, and their interplay, is crucial to understand the mechanism of ejection of mass and disk formation.

6. Conclusions

In this work we used the BCD spectrophotometric system, based on measurable quantities of the stellar continuum spectrum around the Balmer discontinuity, to directly determine the fundamental parameters (spectral type, luminosity class, T_{eff} , $\log g$, M_v , M_{bol} and Φ_b^0) of 68 B and Be stars in four open clusters. In addition, we were able to derive individual values of the stellar distance modulus, color excess $E(B - V)$, luminosity, mass and age for the whole sample. From these measurements we obtained the cluster parameters.

Thus, this work complete the study of the determination of cluster parameters for eleven open clusters (Collinder 223, Hogg 16, NGC 2645, NGC 3114, NGC 3766, NGC 4755, NGC 6025, NGC 6087, NGC 6250, NGC 6383 and NGC 6530), which are summarized in Table 8. Particularly, the distance determinations obtained through the BCD method for NGC 2645, NGC 6087, NGC 6250, and NGC 6383 agree with distance estimates obtained with classical photometric methods.

Table 8. Open cluster parameters derived with the BCD method.

Open cluster	$E(B - V)$ [mag]	$(m_v - M_v)_0$ [mag]	age [Myr]
Collinder 223	0.25 ± 0.03	11.21 ± 0.25	< 25
Hogg 16a	0.26 ± 0.03	8.91 ± 0.26	< 40
Hogg 16b	0.65 ± 0.09	12.78 ± 0.32	10 – 16
NGC 2645	0.54 ± 0.07	12.39 ± 0.30	6 – 14
NGC 3114	0.05 ± 0.01	9.21 ± 0.15	~ 100
NGC 3766	0.25 ± 0.02	11.50 ± 0.15	6 – 28
NGC 4755	0.30 ± 0.04	12.10 ± 0.22	~ 8
NGC 6025	0.34 ± 0.02	9.25 ± 0.17	40 – 68
NGC 6087	0.35 ± 0.03	9.00 ± 0.19	~ 55
NGC 6250	0.38 ± 0.16	10.55 ± 0.33	6
NGC 6383	0.51 ± 0.03	9.61 ± 0.38	3 – 10
NGC 6530	0.26 ± 0.05	11.76 ± 0.20	4 – 6

In addition, from our whole spectroscopic study, we find six new Be stars and fifteen late B stars with circumstellar envelopes out off an emission phase (named Bdd stars). The Be star population represents the 21% of the sample of cluster stars, which is larger than the current population of field Be stars (17%), while the Bdd star group represents $\sim 1/3$ of the Be star population.

We also identify four blue straggler candidates: HD 305 296 (in Collinder 223), NGC 6025 12, NGC 6087 12, and NGC 6530 7.

The maximum distribution of Be stars per spectral subtype presents a maximum at the B2-B4 spectral type in young and intermediate-age open clusters whereas this maximum is at the B6-B8 type in the old clusters. In addition, we find that $\sim 30\%$ of the cluster B stars have circumstellar envelopes (Be + Bdd stars).

Finally, our result supports the statement that the Be phenomenon occurs in very different evolutionary states and occupy the whole main sequence band. On the other hand, we find clearly indication of an enhancement of the Be phenomenon with age which is confirmed by the increase of the fraction number of Be stars at the spectral types B2-B4 in the age interval 10–40 Myr. We also find the appearance of an important number of low massive (later than B4) stars with circumstellar envelopes and out of emission phase (named Bdd stars) in the old open clusters. This last group was detected because of the presence of a second Balmer discontinuity.

Acknowledgements. We would like to thank our anonymous Referee for his/her careful reading and valuable comments and suggestions that certainly help to improve this manuscript. YJA: Visiting Astronomer, Complejo Astronómico El Leoncito operated under agreement between the Consejo Nacional de Investigaciones Científicas y Técnicas de la República Argentina and the National Universities of La Plata, Córdoba and San Juan. This research has made use of the SIMBAD database, operated at CDS, Strasbourg, France, and WEBDA database, operated at the Department of Theoretical Physics and Astrophysics of the Masaryk University. This work was granted by the National University of La Plata (jóvenes investigadores 2016). LC thanks financial support from CONICET (PIP 0177) and the Universidad Nacional de La Plata (Programa de Incentivos G11/137), Argentina.

References

- Aidelman, Y., Cidale, L. S., Zorec, J., & Arias, M. L. 2012, A&A, 544, A64
Aidelman, Y., Cidale, L. S., Zorec, J., & Panei, J. A. 2015, A&A, 577, A45
Aidelman, Y. J., Cidale, L. S., Zorec, J., & Arias, M. L. 2010, Boletín de la Asociación Argentina de Astronomía La Plata Argentina, 53, 141
An, D., Terndrup, D. M., & Pinsonneault, M. H. 2007, ApJ, 671, 1640
Antalová, A. 1972, Bulletin of the Astronomical Institutes of Czechoslovakia, 23, 126
Barbier, D. & Chalonge, D. 1939, ApJ, 90, 627
Battinelli, P. & Capuzzo-Dolcetta, R. 1991, MNRAS, 249, 76
Baumgardt, H., Dettbarn, C., & Wielen, R. 2000, A&AS, 146, 251
Becker, W. & Fenkart, R. 1971, A&AS, 4, 241
Boehm-Vitense, E., Hodge, P., & Boggs, D. 1984, ApJ, 287, 825
Boggs, D. & Boehm-Vitense, E. 1989, ApJ, 339, 209
Breger, M. 1966, PASP, 78, 293
Bruggen, P. & Smeyers, P. 1987, A&A, 186, 170
Chalonge, D. & Divan, L. 1973, A&A, 23, 69
Chini, R. & Neckel, T. 1981, A&A, 102, 171
Cidale, L., Zorec, J., & Tringaniello, L. 2001, A&A, 368, 160
Cidale, L. S., Arias, M. L., Torres, A. F., et al. 2007, A&A, 468, 263
Clariá, J. J. & Lapasset, E. 1991, PASP, 103, 998
Cochetti, Y. R., Arias, M. L., Cidale, L., & Zorec, J. 2013, Boletín de la Asociación Argentina de Astronomía La Plata Argentina, 56, 207
Cochetti, Y. R., Arias, M. L., Cidale, L. S., Granada, A., & Zorec, J. 2015, Boletín de la Asociación Argentina de Astronomía La Plata Argentina, 57, 108
Cook, K. H., Allcock, C., Allsman, H. A., et al. 1995, in Astronomical Society of the Pacific Conference Series, Vol. 83, IAU Colloq. 155: Astrophysical Applications of Stellar Pulsation, ed. R. S. Stobie & P. A. Whitelock, 221
Cox, A. N. & Pilachowski, C. A. 2000, Allen's astrophysical quantities
De Loore, C., Hensberge, H., Sterken, C., et al. 1979, A&A, 78, 287
de Wit, W. J., Lamers, H. J. G. L. M., Marquette, J. B., & Beaulieu, J. P. 2006, A&A, 456, 1027
Dias, W. S., Alessi, B. S., Moitinho, A., & Lépine, J. R. D. 2002, A&A, 389, 871
Dias, W. S., Monteiro, H., Caetano, T. C., et al. 2014, A&A, 564, A79
Didelon, P. 1982, A&AS, 50, 199
Divan, L. 1979, in Recherche Astronomique, Vol. 9, IAU Colloq. 47: Spectral Classification of the Future, ed. M. F. McCarthy, A. G. D. Philip, & G. V. Coyne, 247–256

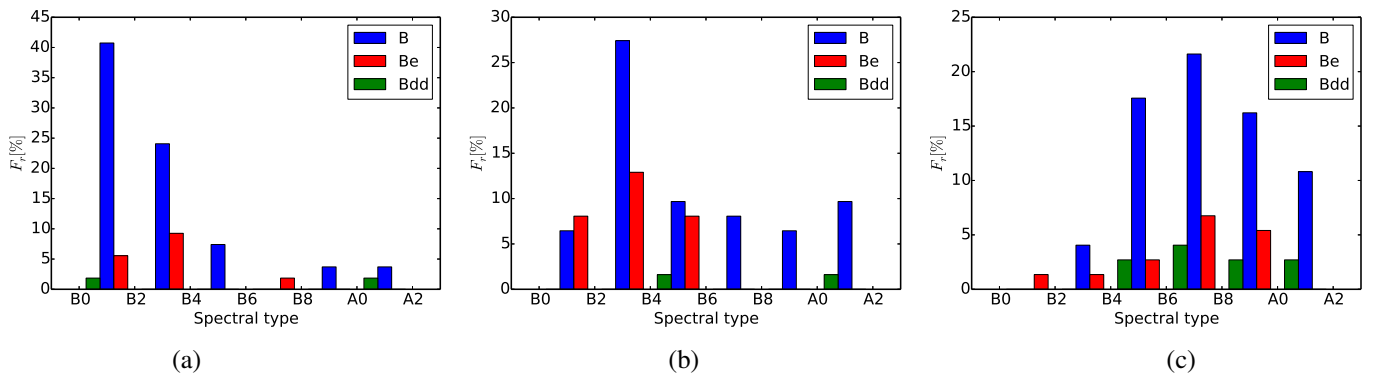


Fig. 16. Number and frequency of stars with and without circumstellar envelopes per spectral subtype in open clusters with different ages: (a) between 3 Myr and 10 Myr, (b) between 10 Myr and 40 Myr, and (c) older than 40 Myr. The plots show a clear trend of the appearance of the Be phenomenon with age.

- Divan, L. & Zorec, J. 1982, in IAU Symposium, Vol. 98, Be Stars, ed. M. Jaschek & H.-G. Groth, 61–63
- Divan, L., Zorec, J., & Andriolat, Y. 1983, *A&A*, 126, L8
- Dufton, P. L., Smartt, S. J., Lee, J. K., et al. 2006, *A&A*, 457, 265
- Eggen, O. J. 1961, *Royal Greenwich Observatory Bulletins*, 27, 61
- Ekström, S., Georgy, C., Eggenberger, P., et al. 2012, *A&A*, 537, A146
- Ekström, S., Meynet, G., Maeder, A., & Barblan, F. 2008, *A&A*, 478, 467
- Fabregat, J. & Torrejón, J. M. 2000, *A&A*, 357, 451
- Feast, M. W. 1957, *MNRAS*, 117, 193
- Feinstein, A. 1994, *Rev. Mexicana Astron. Astrofis.*, 29, 141
- Feinstein, C., Vergne, M. M., Martínez, R., & Orsatti, A. M. 2008, *MNRAS*, 391, 447
- Fernie, J. D. 1961, *ApJ*, 133, 64
- Fitzgerald, M. P., Boudreault, R., Fich, M., Luiken, M., & Witt, A. N. 1979a, *A&AS*, 37, 351
- Fitzgerald, M. P., Jackson, P. D., Luiken, M., Grayzeck, E. J., & Moffat, A. F. J. 1978, *MNRAS*, 182, 607
- Fitzgerald, M. P., Luiken, M., Maitzen, H. M., & Moffat, A. F. J. 1979b, *A&AS*, 37, 345
- Frémat, Y., Zorec, J., Hubert, A., & Floquet, M. 2005, *A&A*, 440, 305
- Gerbaldi, M. & Zorec, J. 1993, in *Astronomical Society of the Pacific Conference Series*, Vol. 40, IAU Colloq. 137: Inside the Stars, ed. W. W. Weiss & A. Baglin, 150
- Ghosh, K. K., Apparao, K. M. V., & Pukalenth, S. 1999, *A&AS*, 134, 359
- Gkouvelis, L., Fabregat, J., Zorec, J., et al. 2016, *A&A*, 591, A140
- Graham, J. A. 1967, *MNRAS*, 135, 377
- Grebel, E. K. 1997, *A&A*, 317, 448
- Harris, G. L. H. 1976, *ApJS*, 30, 451
- Herbst, W. 1977, *AJ*, 82, 902
- Hiltner, W. A., Morgan, W. W., & Neff, J. S. 1965, *ApJ*, 141, 183
- Hubert, A. M., & Floquet, M. 1998, *A&A*, 335, 565
- Hubert, A. M., Floquet, M., & Zorec, J. 2000, in *Astronomical Society of the Pacific Conference Series*, Vol. 214, IAU Colloq. 175: The Be Phenomenon in Early-Type Stars, ed. M. A. Smith, H. F. Henrichs, & J. Fabregat, 348
- Janes, K. & Adler, D. 1982, *ApJS*, 49, 425
- Johnson, H. L., Hoag, A. A., Iriarte, B., Mitchell, R. I., & Hallam, K. L. 1961, *Lowell Observatory Bulletin*, 5, 133
- Keller, S. C., Bessell, M. S., Cook, K. H., Geha, M., & Syphers, D. 2002, *AJ*, 124, 2039
- Kharchenko, N. V., Berczik, P., Petrov, M. I., et al. 2009, *A&A*, 495, 807
- Kharchenko, N. V., Piskunov, A. E., Röser, S., Schilbach, E., & Scholz, R.-D. 2005, *A&A*, 438, 1163
- Kharchenko, N. V., Piskunov, A. E., Schilbach, E., Röser, S., & Scholz, R.-D. 2013, *A&A*, 558, A53
- Kilambi, G. C. 1975, *PASP*, 87, 975
- Kilambi, G. C. 1977, *MNRAS*, 178, 423
- Kumar, B., Sagar, R., Sanwal, B. B., & Bessell, M. S. 2004, *MNRAS*, 353, 991
- Landolt, A. U. 1963, *AJ*, 68, 283
- Landolt, A. U. 1964, *ApJS*, 8, 329
- Landstreet, J. D., Silaj, J., Andretta, V., et al. 2008, *A&A*, 481, 465
- Lindoff, U. 1968, *Arkiv for Astronomi*, 5, 1
- Lloyd Evans, T. 1978, *MNRAS*, 184, 661
- Lodén, L. O. & Nordström, B. 1969, *Arkiv for Astronomi*, 5, 231
- Loktin, A. V. & Beshenov, G. V. 2001, *Astronomy Letters*, 27, 386
- Maitzen, H. M. 1985, *A&AS*, 62, 129
- Malchenko, S. L. 2008, *Odessa Astronomical Publications*, 21, 60
- Martin, A. J., Stift, M. J., Fossati, L., et al. 2017, *MNRAS*, 466, 613
- Martins, F., Schaerer, D., & Hillier, D. J. 2005, *A&A*, 436, 1049
- Mathew, B., Subramaniam, A., & Bhatt, B. C. 2008, *MNRAS*, 388, 1879
- Mayne, N. J. & Naylor, T. 2008, *MNRAS*, 386, 261
- McSwain, M. V. & Gies, D. R. 2005, *ApJS*, 161, 118
- McSwain, M. V., Huang, W., & Gies, D. R. 2009, *ApJ*, 700, 1216
- McSwain, M. V., Huang, W., Gies, D. R., Grundstrom, E. D., & Townsend, R. H. D. 2008, *ApJ*, 672, 590
- Mennickent, R. E., Pietrzyński, G., Gieren, W., & Szewczyk, O. 2002, *A&A*, 393, 887
- Mermilliod, J. C. 1982, *A&A*, 109, 48
- Meynet, G., Mermilliod, J.-C., & Maeder, A. 1993, *A&AS*, 98, 477
- Moffat, A. F. J. & Vogt, N. 1975, *A&AS*, 20, 155
- Moujtahid, A., Zorec, J., & Hubert, A. M. 1999, *A&A*, 349, 151
- Moujtahid, A., Zorec, J., Hubert, A. M., Garcia, A., & Burki, G. 1998, *A&AS*, 129, 289
- Niedzielski, A. & Muciek, M. 1988, *Acta Astron.*, 38, 225
- Ouazzani, R.-M., Dupret, M.-A., & Reese, D. R. 2012, *A&A*, 547, A75
- Pandey, A. K., Bhatt, B. C., Mahra, H. S., & Sagar, R. 1989, *MNRAS*, 236, 263
- Paunzen, E., Netopil, M., & Zwintz, K. 2007, *A&A*, 462, 157
- Penston, M. V. 1964, *The Observatory*, 84, 141
- Piskunov, A. E. 1980, *Bulletin d'Information du Centre de Données Stellaires*, 19, 67
- Piskunov, A. E., Schilbach, E., Kharchenko, N. V., Röser, S., & Scholz, R.-D. 2007, *A&A*, 468, 151
- Piskunov, A. E., Schilbach, E., Kharchenko, N. V., Röser, S., & Scholz, R.-D. 2008, *A&A*, 477, 165
- Prisinzano, L., Damiani, F., Micela, G., & Sciortino, S. 2005, *A&A*, 430, 941
- Rastorguev, A. S., Glushkova, E. V., Dambis, A. K., & Zabolotskikh, M. V. 1999, *Astronomy Letters*, 25, 595
- Rauw, G. & De Becker, M. 2008, *The Multiwavelength Picture of Star Formation in the Very Young Open Cluster NGC 6383*, ed. B. Reipurth, 497
- Robichon, N., Arenou, F., Mermilliod, J.-C., & Turon, C. 1999, *A&A*, 345, 471
- Sagar, R. 1987, *MNRAS*, 228, 483
- Sagar, R. & Cannon, R. D. 1997, *A&AS*, 122, 9
- Sagar, R. & Joshi, U. C. 1978, *MNRAS*, 184, 467
- Sagar, R., Piskunov, A. E., Miakutin, V. I., & Joshi, U. C. 1986, *MNRAS*, 220, 383
- Sahade, J. & Berón Dávila, F. 1963, *Annales d'Astrophysique*, 26, 153
- Sanford, R. F. 1949, *ApJ*, 110, 117
- Schmidt, E. G. 1980, *AJ*, 85, 158
- Shimazaki, H. & Shinomoto, S. 2007, *Neural Computation*, 19, 1503
- Shobbrook, R. R. 1985, *MNRAS*, 212, 591
- Sletbak, A. 1985, *ApJS*, 59, 769
- Sota, A., Maíz Apellániz, J., Walborn, N. R., et al. 2011, *ApJS*, 193, 24
- Strobel, A., Skaba, W., & Proga, D. 1992, *A&AS*, 93, 271
- Sung, H., Chun, M.-Y., & Bessell, M. S. 2000, *AJ*, 120, 333
- The, P.-S. 1965, *Contributions from the Bosscha Observatory*, 32, 0
- The, P.-S. 1966, *Contributions from the Bosscha Observatory*, 34, 1
- The, P. S., Hageman, T., Tjin A Djie, H. R. E., & Westerlund, B. E. 1985, *A&A*, 151, 391
- Torres, A. V. 1987, *ApJ*, 322, 949
- Tosi, M. 1979, *Mem. Soc. Astron. Italiana*, 50, 245
- Trumpler, R. J. 1930, *Lick Observatory Bulletin*, 14, 154
- Turner, D. G. 1986, *AJ*, 92, 111
- van Altena, W. F. 1972, *ApJ*, 178, L127
- van den Ancker, M. E., Thé, P. S., & de Winter, D. 2000, *A&A*, 362, 580
- van den Ancker, M. E., Thé, P. S., Feinstein, A., et al. 1997, *A&AS*, 123, 63
- Vinicius, M. M. F., Zorec, J., Leister, N. V., & Levenhagen, R. S. 2006, *A&A*, 446, 643

- Walker, M. F. 1957, ApJ, 125, 636
- Wright, E. L., Eisenhardt, P. R. M., Mainzer, A. K., et al. 2010, AJ, 140, 1868
- Zhao, J.-L., Chen, L., & Wen, W. 2006, Chinese J. Astron. Astrophys., 6, 435
- Zorec, J. 1986, Thèse d'État: Structure et rotation différentielle dans les étoiles B avec et sans émission (Université Paris VII)
- Zorec, J. & Briot, D. 1991, A&A, 245, 150
- Zorec, J. & Briot, D. 1997, A&A, 318, 443
- Zorec, J., Cidale, L., Arias, M. L., et al. 2009, A&A, 501, 297
- Zorec, J., Divan, L., & Hoeflich, P. 1989, A&A, 210, 279
- Zorec, J., Frémat, Y., & Cidale, L. 2005, A&A, 441, 235
- Zorec, J., Frémat, Y., Cidale, L. S., Chauville, J., & Ballereau, D. 2003, Boletín de la Asociación Argentina de Astronomía La Plata Argentina, 46, 30
- Zorec, J., Frémat, Y., Domiciano de Souza, A., et al. 2016, A&A, Enviado
- Zug, R. S. 1937, Lick Observatory Bulletin, 18, 89

Table 1. Log of observations of low-resolution spectra. The coordinates α and δ correspond to the ICRS system (ep = J2000 and eq = 2000). *AM* is the air mass and *N* is the number of spectra taken for each star with the Boller & Chivens spectrograph. Nomenclatures for NGC 6087 corresponds to Fernie (1961) and Breger (1966), for NGC 6250 to Moffat & Vogt (1975) and Herbst (1977), for NGC 6383 to Eggen (1961); The (1965) and Lloyd Evans (1978), and for NGC 6530 to Walker (1957) and Kilambi (1977).

ID	Other designation	α	δ	<i>AM</i>	dates	<i>N</i>
NGC 6087						
001	HD 146 271	16 : 18 : 37.60	-57 : 41 : 46.06	1.18	2013-07-20	1
007	HD 146 483	16 : 19 : 38.46	-57 : 54 : 22.57	1.1, 1.1, 1.14	2003-04-26, 2003-06-04, 2013-07-22	3
008	HD 146 448	16 : 19 : 25.14	-57 : 53 : 08.59	1.3	2003-04-25	1
009	HD 146 484	16 : 19 : 36.67	-57 : 56 : 05.46	1.1, 1.1, 1.13	2003-04-26, 2003-06-04, 2013-07-22	3
010	HD 146 324	16 : 18 : 49.01	-57 : 55 : 51.52	1.1, 1.17	2003-04-25, 2013-07-20	2
011	HD 146 294	16 : 18 : 37.89	-57 : 56 : 20.30	1.1	2003-04-25	2
013	HD 146 261	16 : 18 : 24.89	-57 : 49 : 32.97	1.14	2013-07-20	1
014	CPD-57 7791	16 : 18 : 22.81	-57 : 51 : 28.67	1.2	2003-04-26	1
015	HD 146 204	16 : 18 : 06.40	-57 : 51 : 00.39	1.2	2003-04-26	1
022	HD 146 531	16 : 19 : 55.47	-58 : 10 : 01.87	1.16	2013-07-20	1
025	CPD-57 7817	16 : 18 : 49.69	-57 : 54 : 30.31	1.1	2003-04-25	1
033	GEN# +2.60870033	16 : 19 : 47.00	-57 : 56 : 12.00	1.1	2003-06-04	1
035	HD 146 428	16 : 19 : 21.24	-57 : 54 : 23.72	1.2	2003-04-25	1
036	GEN# +2.60870036	16 : 19 : 20.00	-57 : 52 : 18.00	1.2	2003-04-25	1
101	GEN# +2.60870101	16 : 18 : 16.62	-57 : 48 : 42.76	1.2	2003-04-26	1
128	CD-57 6341	16 : 18 : 50.58	-57 : 56 : 39.71	1.1	2003-04-25	1
129	GEN# +2.60870129	16 : 18 : 47.06	-57 : 56 : 44.89	1.1	2003-04-25	1
156	CD-57 6346	16 : 19 : 18.33	-57 : 53 : 36.54	1.1	2003-04-25	1
NGC 6250						
001	HD 152 853	16 : 58 : 07.93	-45 : 58 : 56.47	1.25	2011-05-12	1
002	HD 152 799	16 : 57 : 42.84	-45 : 57 : 41.26	1.2	2011-05-12	1
003	HD 152 822	16 : 57 : 55.89	-45 : 56 : 09.27	1.14	2011-05-12	1
004	HD 152 917	16 : 58 : 33.03	-45 : 55 : 13.28	1.25, 1.08	2011-05-13, 2013-07-21	2
017	HD 329 271	16 : 57 : 41.27	-45 : 58 : 49.91	1.04	2013-07-21	1
018	CD-45 11088	16 : 57 : 43.04	-46 : 00 : 27.09	1.03	2011-05-12	1
021	HD 152 743	16 : 57 : 20.45	-45 : 51 : 57.87	1.09	2011-05-13	1
022	HD 152 706	16 : 57 : 12.10	-45 : 52 : 35.73	1.14	2011-05-13	1
032	HD 152 687	16 : 57 : 04.46	-46 : 08 : 37.49	1.2	2011-05-13	1
033	HD 152 561	16 : 56 : 15.54	-46 : 02 : 57.73	1.03	2011-05-13	1
034	HD 153 073	16 : 59 : 26.70	-45 : 53 : 04.29	1.06	2011-05-13	1
035	HD 152 979	16 : 58 : 56.81	-46 : 07 : 44.38	1.04	2011-05-12	1
037	HD 329 379	17 : 01 : 05.88	-45 : 42 : 04.32	1.04, 1.09	2011-05-13, 2013-07-21	2
...	CD-49 11096	16 : 59 : 36.86	-49 : 45 : 25.45	1.2	2013-07-23	1
...	HD 329 211	16 : 59 : 32.55	-44 : 52 : 37.52	1.08	2011-05-12	1
NGC 6383						
001	CD-32 12935	17 : 34 : 42.49	-32 : 34 : 53.99	1.03, 1.0, 1.12	2012-06-06, 2012-06-08, 2013-07-21	3
002	CD-32 12931	17 : 34 : 34.95	-32 : 33 : 47.13	1.46	2012-06-08	1
003	CD-32 12927	17 : 34 : 34.20	-32 : 36 : 08.90	1.	2012-06-08	1
006	CD-32 12921	17 : 34 : 22.02	-32 : 33 : 38.85	1.04, 1.02	2012-06-06, 2012-06-08	2
010	CD-32 12943	17 : 34 : 57.22	-32 : 40 : 20.92	1.11	2012-06-08	1
014	CD-32 12929	17 : 34 : 38.56	-32 : 34 : 59.30	1.27	2012-06-07	1
047	CD-32 12954	17 : 35 : 10.24	-32 : 29 : 04.08	1.06	2012-06-08	1
057	CD-32 12946	17 : 35 : 02.16	-32 : 37 : 36.30	1.25	2013-07-23	1
076	CD-32 12908	17 : 34 : 02.23	-32 : 40 : 39.68	1.	2012-06-07	1
083	CD-32 12919	17 : 34 : 16.86	-32 : 36 : 32.06	1.02	2012-06-07	1
085	CD-32 12910	17 : 34 : 02.69	-32 : 37 : 49.14	1.06	2012-06-07	1
100	CD-32 12924	17 : 34 : 24.51	-32 : 30 : 15.98	1.09, 1.03	2012-06-06, 2012-06-08	2
NGC 6530						
007	HD 164 794	18 : 03 : 52.44	-24 : 21 : 38.63	1.22, 1.18	2012-06-06, 2013-07-21	2
009	HD 164 816	18 : 03 : 56.87	-24 : 18 : 45.22	1.3	2011-05-12	1
032	GEN# +2.65300032	18 : 04 : 11.16	-24 : 21 : 45.20	1.01	2011-05-10	1
042	HD 315 032	18 : 04 : 15.03	-24 : 23 : 27.71	1.01	2011-05-10	1
043	HD 315 026	18 : 04 : 14.51	-24 : 14 : 37.02	1.26	2011-05-13	1
045	HD 164 865	18 : 04 : 15.22	-24 : 11 : 00.09	1.14, 1.2	2011-05-11, 2013-07-21	2
055	HD 315 023	18 : 04 : 20.56	-24 : 13 : 54.90	1.01	2011-05-12	1

Continued on next page.

Table 1 – *Continued from previous page.*

ID	Other designation	α	δ	AM	dates	N
056	CD–24 13829	18 : 04 : 21.30	–24 : 21 : 18.18	1.02	2011-05-10	1
059	HD 315 033	18 : 04 : 23.23	–24 : 26 : 16.71	1.22, 1.18	2011-05-11, 2013-07-20	2
060	LSS 4615	18 : 04 : 24.00	–24 : 21 : 26.70	1.04	2011-05-10	1
061	ALS 16976	18 : 04 : 24.29	–24 : 20 : 59.50	1.08	2011-05-10	1
065	HD 164 906	18 : 04 : 25.84	–24 : 23 : 08.35	1.09	2011-05-09	1
066	CD–24 13831	18 : 04 : 25.55	–24 : 20 : 45.00	1.03	2011-05-11	1
068	CD–24 13830	18 : 04 : 22.74	–24 : 22 : 09.80	1.01, 1.24	2011-05-11, 2013-07-21	2
070	ALS 18783	18 : 04 : 27.21	–24 : 22 : 49.56	1.05	2011-05-12	1
073	HD 315 031	18 : 04 : 28.05	–24 : 21 : 42.98	1.14	2011-05-09	1
076	HD 315 024	18 : 04 : 29.28	–24 : 19 : 25.37	1.03	2011-05-13	1
080	CD–24 13837	18 : 04 : 32.99	–24 : 23 : 12.52	1.15	2011-05-13	1
085	HD 164 933	18 : 04 : 33.03	–24 : 09 : 38.27	1.1	2011-05-11	1
086	CD–24 13840	18 : 04 : 34.20	–24 : 22 : 00.60	1.17	2011-05-12	1
093	HD 315 021	18 : 04 : 36.00	–24 : 19 : 52.19	1.27	2011-05-09	1
100	HD 164 947	18 : 04 : 41.66	–24 : 20 : 56.95	1.12, 1.33	2012-06-06, 2012-06-06	2
...	LSS 4627	18 : 04 : 41.03	–21 : 04 : 52.33	1.06	2011-05-13	1

Table 2. Log of high-resolution spectra observations. The coordinates α and δ correspond to the ICRS system (ep = J2000 and eq = 2000). X indicates the values of the air mass of star. The last column, N , lists the number of spectra taken for each star with the REOSC DC spectrograph. Clusters NGC 3766 and NGC 4755 were published in Paper I, Collinder 223, Hogg 16, NGC 3114, and NGC 6025 were published in Paper II.

ID	α	δ	AM	dates	N
Collinder 223					
002	10 : 29 : 33.699	-60 : 12 : 37.42	1.15	2013-04-22	1
080	10 : 30 : 23.8684	-60 : 04 : 40.429	1.21	2013-04-22	1
106	10 : 30 : 20.3124	-60 : 01 : 48.515	1.17	2013-04-22	1
HD 305 296	10 : 31 : 39.8575	-60 : 17 : 10.938	1.14	2013-04-23	1
Hogg 16					
003	13 : 29 : 34.28722	-61 : 11 : 36.1245	1.20	2013-04-22	1
009	13 : 29 : 17.565	-61 : 11 : 51.84	1.20	2013-04-24	1
014	13 : 29 : 09.1238	-61 : 05 : 41.931	1.15	2013-06-22	1
052	13 : 28 : 43.9231	-61 : 01 : 25.820	1.15	2013-04-22	1
068	13 : 28 : 01.49589	-61 : 03 : 45.0368	1.15	2013-04-22	1
NGC 2645					
01	08 : 39 : 04.174	-46 : 13 : 36.51	1.03	2013-04-21	1
04	08 : 39 : 05.711	-46 : 14 : 45.44	1.04	2013-04-21	1
05	08 : 39 : 04.341	-46 : 14 : 52.09	1.06	2013-04-22	1
NGC 3114					
003	10 : 03 : 08.21073	-59 : 50 : 27.8712	1.17	2013-04-23	1
004	10 : 01 : 41.76408	-60 : 06 : 46.5882	1.14	2013-04-23	1
011	10 : 00 : 21.091	-59 : 59 : 52.59	1.14	2013-04-24	1
015	10 : 04 : 08.9394	-59 : 52 : 54.735	1.14	2013-04-24	1
028	10 : 02 : 48.9721	-59 : 50 : 18.995	1.20	2013-04-23	1
033	10 : 05 : 39.7720	-60 : 00 : 37.716	1.18	2013-04-24	1
047	10 : 03 : 50.7764	-59 : 51 : 23.325	1.15	2013-04-24	1
091	10 : 00 : 57.517	-59 : 58 : 23.81	1.24	2013-04-24	1
129	10 : 02 : 35.580	-60 : 08 : 51.49	1.16	2013-04-23	1
HD 87 801	10 : 05 : 33.4110	-59 : 54 : 23.665	1.17	2013-04-23	1
NGC 3766					
026	11 : 36 : 09.565	-61 : 35 : 38.20	1.20	2013-04-23	1
027	11 : 36 : 11.903	-61 : 35 : 50.05	1.18	2013-04-23	1
151	11 : 36 : 12.35	-61 : 32 : 44.9	1.16	2013-04-23	1
232	11 : 36 : 28.37117	-61 : 39 : 54.5183	1.24	2013-04-24	1
239	11 : 36 : 09.36848	-61 : 41 : 41.5868	1.17	2013-06-23	1
240	11 : 36 : 05.48263	-61 : 42 : 06.0590	1.20	2013-06-21	1
264	11 : 35 : 15.1721	-61 : 41 : 59.607	1.16	2013-06-21	1
291	11 : 35 : 22.0682	-61 : 32 : 11.048	1.21	2013-06-23	1
301	11 : 37 : 48.854	-61 : 45 : 05.15	1.17	2013-06-24	1
HD 306 787	11 : 36 : 48.37	-61 : 26 : 41.7	1.24	2013-06-25	1
HD 308 852	11 : 37 : 41.9600	-61 : 45 : 42.733	1.19	2013-04-24	1
NGC 4755					
001	12 : 53 : 21.89463	-60 : 19 : 42.5630	1.18	2013-04-23	1
106	12 : 53 : 37.62181	-60 : 21 : 25.3912	1.17	2013-04-23	1
306	12 : 53 : 51.57	-60 : 23 : 16.9	1.18	2013-04-24	1
NGC 6025					
01	16 : 03 : 44.46671	-60 : 29 : 54.4704	1.18	2013-04-22	1
03	16 : 03 : 28.89312	-60 : 29 : 12.7768	1.16	2013-04-22	1
25	16 : 03 : 31.9865	-60 : 20 : 11.228	1.15	2013-04-22	1
NGC 6087					
007	16 : 19 : 38.4600	-57 : 54 : 22.571	1.12	2013-04-22	1
009	16 : 19 : 36.6658	-57 : 56 : 05.457	1.11	2013-04-22	1
010	16 : 18 : 49.0134	-57 : 55 : 51.524	1.17, 1.11	2013-04-22, 2013-04-24	2
011	16 : 18 : 37.8903	-57 : 56 : 20.299	1.16	2013-04-23	1
014	16 : 18 : 22.8167	-57 : 51 : 28.668	1.13	2013-04-23	1
156	16 : 19 : 18.329	-57 : 53 : 36.54	1.11	2013-04-23	1
NGC 6250					
01	16 : 58 : 07.92884	-45 : 58 : 56.4699	1.05	2013-06-22	1
02	16 : 57 : 42.84338	-45 : 57 : 41.2602	1.04	2013-06-22	1

Continued on next page.

Table 2 – *Continued from previous page.*

ID	α	δ	AM	dates	N
03	16 : 57 : 55.891	–45 : 56 : 09.27	1.03	2013-06-22	1
17	16 : 57 : 41.2747	–45 : 58 : 49.914	1.07	2013-06-24	1
32	16 : 57 : 04.45812	–46 : 08 : 37.4944	1.04	2013-06-22	1
33	16 : 56 : 15.5437	–46 : 02 : 57.727	1.05	2013-06-22	1
35	16 : 58 : 56.80575	–46 : 07 : 44.3797	1.07	2013-06-25	1
NGC 6383					
001	17 : 34 : 42.49348	–32 : 34 : 53.9926	1.00	2013-04-23	1
047	17 : 35 : 10.244	–32 : 29 : 04.08	1.01	2013-04-23	1
076	17 : 34 : 02.227	–32 : 40 : 39.68	1.00	2013-04-24	1
100	17 : 34 : 24.51266	–32 : 30 : 15.9812	1.02, 1.07	2013-04-24, 2013-06-24	2
NGC 6530					
009	18 : 03 : 56.866	–24 : 18 : 45.22	1.21	2013-06-24	1
032	18 : 04 : 11.16	–24 : 21 : 45.2	1.01	2013-06-25	1
042	18 : 04 : 15.02620	–24 : 23 : 27.7087	1.03	2013-06-25	1
045	18 : 04 : 15.2176	–24 : 11 : 00.090	1.12	2013-06-25	1
055	18 : 04 : 20.56	–24 : 13 : 54.9	1.09	2013-06-24	1
086	18 : 04 : 34.20	–24 : 22 : 00.6	1.11	2013-06-25	1
100	18 : 04 : 41.658	–24 : 20 : 56.95	1.32	2013-06-25	1

Table 9. NGC 6087: Stellar fundamental parameters from the BCD system. Nomenclature according to Fernie (1961) and Breger (1966).

ID	Other	D	λ_1	Φ_b	S.T	T_{eff}	$\log g$	M_v	M_{bol}	Φ_b^0
Fernie/ Breger	designation	[dex]	[Å]	[μ]		[K]	[dex]	[mag]	[mag]	[μ]
001	HD 146 271	0.23	45	1.37	B4IV	16 971 ± 744	3.61 ± 0.31	-1.81 ± 0.52	-3.10 ± 0.48	0.75 ± 0.01
007	HD 146 483 ^{dd}	0.30	55	1.18	B6Ve	14 162 ± 521	4.11 ± 0.17	-0.41 ± 0.22	-1.44 ± 0.29	0.79 ± 0.01
008	HD 146 448	0.26	53	1.14	B5V	15 765 ± 600	4.01 ± 0.21	-0.94 ± 0.35	-2.09 ± 0.33	0.77 ± 0.01
009	HD 146 484 ^{dd}	0.30	61	1.13	B6Ve ^{Be}	13 810 ± 511	4.24 ± 0.10	-0.31 ± 0.26	-1.31 ± 0.23	0.80 ± 0.02
010	HD 146 324 ^{dd}	0.26	44	1.39	B5IIIe ^{Be}	16 250 ± 631	3.58 ± 0.31	-1.69 ± 0.51	-2.75 ± 0.46	0.76 ± 0.01
011	HD 146 294 ^{dd}	0.24	53	1.25	B4V	16 604 ± 782	4.00 ± 0.22	-1.29 ± 0.37	-2.50 ± 0.37	0.75 ± 0.01
013	HD 146 261	0.26	53	1.37	B5V	16 159 ± 506	4.01 ± 0.21	-1.07 ± 0.36	-2.24 ± 0.34	0.76 ± 0.01
014	CPD-57 7791 ^{dd}	0.35	58	1.10	B8V ^{Be}	12 273 ± 447	4.20 ± 0.11	0.03 ± 0.25	-0.84 ± 0.21	0.83 ± 0.02
015	HD 146 204	0.30	59	1.23	B6V	14 783 ± 663	4.22 ± 0.13	-0.35 ± 0.26	-1.39 ± 0.22	0.79 ± 0.01
022	HD 146 531	0.18	53	1.35	B2IVe ^{Be}	20 945 ± 1 236	3.92 ± 0.26	-2.16 ± 0.41	-3.77 ± 0.40	0.72 ± 0.01
025	CPD-57 7817	0.30	64	1.26	B7V ^{CP2}	13 879 ± 485	4.33 ± 0.10	-0.41 ± 0.19	-1.30 ± 0.19	0.80 ± 0.02
033	GEN# +2.60870033	0.52	71	1.10	A2:V:	9 063 ± 348:	4.34 ± 0.10:	1.15 ± 0.50:	1.10 ± 0.27 ^a	1.14 ± 0.06
035	HD 146 428	0.37	77	1.79	A8:VI:	7 652 ± 176 ^a	4.32 ± 0.01 ^a	2.40 ± 0.15 ^a	2.29 ± 0.15 ^a	1.54 ± 0.03
036	GEN# +2.60870036	0.32	57	1.30	B6V	13 673 ± 592	4.17 ± 0.14	-0.27 ± 0.23	-1.16 ± 0.24	0.80 ± 0.01
101	GEN# +2.60870101 ^{dd}	0.44	73	1.10	A1:VI:	10 355 ± 336:	4.50 ± 0.10:	0.50 ± 0.43:	0.73 ± 0.32 ^a	1.00 ± 0.04
128	CD-57 6341	0.23	49	1.41	B4IV	17 694 ± 779	3.82 ± 0.27	-1.60 ± 0.47	-3.04 ± 0.45	0.75 ± 0.01
129	GEN# +2.60870129	0.49	72	1.60	A2:V:	10 137 ± 625:	4.41 ± 0.10:	1.15 ± 0.50:	1.10 ± 0.27 ^a	1.10 ± 0.07
156	CD-57 6346 ^{dd}	0.26	71	1.06	B6:V:	15 605 ± 761:	4.35 ± 0.05:	-0.95 ± 0.16:	-1.89 ± 0.20:	0.78 ± 0.02

Notes. The symbol : is used to indicate extrapolated values. g is the stellar surface gravity given in cm s^{-2} . (^{dd}) Star with a SBD. (^{Be}) Known Be star. (^{CP2}) Chemically peculiar star. (^a) Values interpolated from Cox & Pilachowski (2000).

Table 10. NGC 6087: Physical parameters and distance to the stars.

ID	Other	m_v	$E(B - V)$	$(m_v - M_v)_0$	AD	p	$\log \mathcal{L}_\star$	M_\star	age
Fernie/ Breger	designation	[mag]	[mag]	[mag]	[arcmin]	[%]	[\mathcal{L}_\odot]	[M_\odot]	[Myr]
001	HD 146 271	8.35	0.46 ± 0.01	8.7 ± 0.5	14.43	2.1	3.3 ± 0.4	6 ± 1	45 ± 9
007	HD 146 483 ^{dd}	8.29	0.26 ± 0.01	7.9 ± 0.2 ^{pm}	6.66	0.0	2.5 ± 0.3	4 ± 0.2	74 ± 27
008	HD 146 448	9.02	0.28 ± 0.01	9.1 ± 0.4	5.53	40.8	2.8 ± 0.3	5 ± 0.4	55 ± 15
009	HD 146 484 ^{dd}	9.48	0.23 ± 0.01	9.1 ± 0.3	6.19	40.8	2.3 ± 0.2	4 ± 0.2	64 ± 37
010	HD 146 324 ^{dd}	7.92	0.43 ± 0.01	8.3 ± 0.5	0.27	0.0	3.2 ± 0.4	6 ± 1	51 ± 10
011	HD 146 294 ^{dd}	9.43	0.38 ± 0.01	9.6 ± 0.4	1.62	0.0	2.9 ± 0.3	5 ± 0.4	46 ± 13
013	HD 146 261	9.39	0.46 ± 0.01	9.0 ± 0.4	7.35	100.0	2.9 ± 0.3	5 ± 0.4	49 ± 13
014	CPD-57 7791 ^{dd}	9.70	0.20 ± 0.02	9.0 ± 0.3	5.87	100.0	2.1 ± 0.2	3 ± 0.2	121 ± 53
015	HD 146 204	10.19	0.33 ± 0.01	9.5 ± 0.3	7.71	0.1	2.5 ± 0.2	4 ± 0.2	41 ± 27
022	HD 146 531	9.69	0.48 ± 0.01	10.4 ± 0.4 ^{pm}	16.40	0.0	3.5 ± 0.4	8 ± 1	19 ± 7
025	CPD-57 7817	9.82	0.34 ± 0.01	9.2 ± 0.2	1.60	10.8	2.3 ± 0.2	4 ± 0.2	48 ± 42
033	GEN# +2.60870033	11.97	...	6.5 ± 0.2 ^{nm}	7.57	0.0	1.3 ± 0.3	2 ± 0.1	264 ± 240
035	HD 146 428	9.95	0.14 ± 0.02	7.1 ± 0.2 ^{nm}	4.49	0.0	0.9 ± 0.2	2 ± 0.1	458 ± 459
036	GEN# +2.60870036	10.36	0.38 ± 0.01	9.5 ± 0.2	5.51	0.1	2.3 ± 0.2	4 ± 0.2	75 ± 35
101	GEN# +2.60870101 ^{dd}	11.25	0.05 ± 0.01	10.6 ± 0.4 ^{pm}	8.62	0.0	1.4 ± 0.3	2 ± 0.2	103 ± 121
128	CD-57 6341	8.71	0.50 ± 0.01	8.8 ± 0.5	0.57	10.8	3.2 ± 0.4	6 ± 0.6	39 ± 7
129	GEN# +2.60870129	9.75	0.27 ± 0.04	7.8 ± 0.5 ^{pm}	0.76	0.0	1.4 ± 0.3	2 ± 0.1	78 ± 121
156	CD-57 6346 ^{dd}	9.14	0.20 ± 0.01	9.5 ± 0.2	4.51	0.1	2.5 ± 0.2	4 ± 0.3	26 ± 28

Notes. m_v values obtained from SIMBAD database. The distances of the stars with negative color gradients were determined using the distance modulus assigned to the cluster. (^{dd}) Stars with a SBD. (^{pm}) Probable member stars. (^{nm}) Non-member stars.

Table 11. NGC 6250: Stellar fundamental parameters from the BCD system. Nomenclature according to Moffat & Vogt (1975) and Herbst (1977).

ID Moffat/ Herbst	Other designation	D [dex]	λ_1 [Å]	Φ_b [μ]	S.T	T_{eff} [K]	$\log g$ [dex]	M_v [mag]	M_{bol} [mag]	Φ_b^0 [μ]
01	HD 152 853 ^{dd}	0.09	52	1.03	B0III	28 418 ± 2 781	3.47 ± 0.39	-3.75 ± 0.60	-5.91 ± 0.50	0.69 ± 0.00
02	HD 152 799	0.16	76	0.73	B2VI:	22 919 ± 1 577	4.31 ± 0.04:	-1.86 ± 0.15:	-3.72 ± 0.38:	0.71 ± 0.01
03	HD 152 822	0.22	68	0.93	B4VI: ^{VB}	18 236 ± 625	4.30 ± 0.07	-1.32 ± 0.11	-2.62 ± 0.26	0.75 ± 0.01
04	HD 152 917	0.33	70	1.63	F1V	6 930 ± 70 ^a	4.34 ± 0.00 ^a	3.58 ± 0.02 ^a	3.46 ± 0.02 ^a	1.71 ± 0.07
17	HD 329 271	0.22	64	1.36	B4V	18 074 ± 623	4.26 ± 0.09	-1.27 ± 0.19	-2.44 ± 0.32	0.75 ± 0.01
18	CD-45 11088	0.42	70	0.78	A0VI:	10 828 ± 367	4.41 ± 0.11:	0.19 ± 0.38	0.24 ± 0.35:	0.94 ± 0.04
21	HD 152 743	0.12	52	0.75	B1IV	24 600 ± 2 371	3.76 ± 0.34	-3.12 ± 0.52	-5.20 ± 0.47	0.70 ± 0.01
22	HD 152 706	0.46	71	0.79	A1V	10 084 ± 376	4.40 ± 0.10:	0.46 ± 0.25:	0.65 ± 0.36:	1.01 ± 0.04
32	HD 152 687	0.44	58	1.03	B9Ve	10 722 ± 275	4.10 ± 0.16	0.59 ± 0.22:	-0.31 ± 0.33:	0.92 ± 0.03
33	HD 152 561	0.41	56	1.04	B9Ve	11 420 ± 284	4.10 ± 0.16	0.27 ± 0.25	-0.58 ± 0.28	0.88 ± 0.02
34	HD 153 073	0.08	61	0.90	B0V ^p	31 435 ± 1 884	4.01 ± 0.24	-3.46 ± 0.41	-6.19 ± 0.44	0.67 ± 0.01
35	HD 152 979	0.09	57	0.99	B0IVe ^{Be}	31 127 ± 2 571	3.89 ± 0.30	-3.59 ± 0.56	-6.12 ± 0.47	0.68 ± 0.01
37	HD 329 379	0.06	48	2.50	B0II	30 363 ± 4 229	2.92 ± 0.34	-5.11 ± 0.88	-7.26 ± 0.54	0.67 ± 0.01
...	CD-49 11096	0.40	62	1.59	B9V	11 450 ± 308	4.26 ± 0.14	0.46 ± 0.39	-0.34 ± 0.29:	0.89 ± 0.03
...	HD 329 211	0.26	69	0.51	B5VI:	15 747 ± 671	4.34 ± 0.07:	-0.95 ± 0.13	-1.90 ± 0.18	0.77 ± 0.02

Notes. The symbol : is used to indicate extrapolated values. g is the stellar surface gravity given in cm s^{-2} . ^(dd) Stars with a SBD. ^(Be) Known Be star. ^(VB) Reported as visual binary star. ^(p) Chemically peculiar star. ^(a) Values interpolated from Cox & Pilachowski (2000).

Table 12. NGC 6250: Physical parameters and distance to the stars.

ID Moffat Herbst	Other designation	m_v [mag]	$E(B-V)$ [mag]	$(m_v - M_v)_0$ [mag]	AD [arcmin]	p [%]	$\log \mathcal{L}_\star$ [\mathcal{L}_\odot]	M_\star [M_\odot]	age [Myr]
01	HD 152 853 ^{dd}	7.94	0.25 ± 0.01	10.9 ± 0.6	2.91	15.4	4.7 ± 0.6	20 ± 12	6 ± 3
02	HD 152 799	8.74	0.01 ± 0.01	10.6 ± 0.1	2.85	83.3	3.4 ± 0.3	8 ± 1	2 ± 4
03	HD 152 822	9.07	0.14 ± 0.01	9.0 ± 0.1	0.58	3.3	2.9 ± 0.2	6 ± 0.3	11 ± 11
04	HD 152 917	7.62	...	2.9 ± 0.5 ^{nm}	6.24	0.0	0.5 ± 0.1	1 ± 0.1	6 ± 6
17	HD 329 271	10.65	0.46 ± 0.01	10.5 ± 0.2	3.67	83.3	2.9 ± 0.3	5 ± 0.3	12 ± 11
18	CD-45 11088	11.10	...	9.7 ± 0.6	4.65	0.3	1.6 ± 0.3	3 ± 0.2	110 ± 112
21	HD 152 743	9.06	0.04 ± 0.01	12.1 ± 0.5 ^{pm}	8.01	0.0	4.1 ± 0.4	12 ± 2	12 ± 5
22	HD 152 706	10.09	...	8.5 ± 0.6 ^{pm}	8.93	0.0	1.5 ± 0.3	2 ± 0.2	148 ± 152
32	HD 152 687	8.69	0.08 ± 0.02	7.9 ± 0.2 ^{pm}	15.20	0.0	1.9 ± 0.3	3 ± 0.2	236 ± 59
33	HD 152 561	9.11	0.12 ± 0.02	8.5 ± 0.3 ^{pm}	18.90	0.0	2.1 ± 0.3	3 ± 0.2	184 ± 46
34	HD 153 073	9.10	0.17 ± 0.01	12.0 ± 0.4 ^{pm}	15.82	0.0	4.5 ± 0.4	17 ± 3	3 ± 2
35	HD 152 979	8.16	0.23 ± 0.01	11.0 ± 0.6	15.11	7.3	4.6 ± 0.4	17 ± 4	4 ± 3
37	HD 329 379	9.70	1.37 ± 0.01	10.6 ± 0.9	35.81	83.3
...	CD-49 11096	10.91	0.53 ± 0.02	8.8 ± 0.4 ^{pm}	229.43	0.0	1.9 ± 0.3	3 ± 0.2	135 ± 80
...	HD 329 211	10.91	...	10.7 ± 0.5	66.09	52.9	2.6 ± 0.2	4 ± 0.3	24 ± 25

Notes. m_v values obtained from SIMBAD database. The distances of the stars with negative color gradients were determined using the distance modulus assigned to the cluster. ^(dd) Stars with a SBD. ^(pm) Probable member star. ^(nm) Non-member star.

Table 13. NGC 6383: Stellar fundamental parameters from the BCD system. Nomenclature according to Eggen (1961); The (1965), and Lloyd Evans (1978).

ID	Other	D	λ_1	Φ_b	S.T	T_{eff}	$\log g$	M_v	M_{bol}	Φ_b^0
Eggen/The/ Lloyd Evans	designation	[dex]	[Å]	[μ]		[K]	[dex]	[mag]	[mag]	[μ]
001	CD–32 12935	0.01	38	1.37	O7V ^{BE2, BEc, Em, mk}	$38\,000 \pm 2\,000^a$	3.97 ± 0.02^a	-5.10 ± 0.30^a	-8.96 ± 0.30^a	0.62 ± 0.02^m
002	CD–32 12931	0.14	67	1.58	B2V	$24\,678 \pm 1\,125$	4.21 ± 0.08	-2.13 ± 0.27	-4.16 ± 0.31	0.70 ± 0.01
003	CD–32 12927	0.39	96	1.84	A3V ^{VB, BE, MA, mk}	$8\,727 \pm 273^a$	4.23 ± 0.03^a	1.52 ± 0.22^a	1.33 ± 0.22^a	1.12 ± 0.02
006	CD–32 12921	0.07	47	1.43	B0II ^{V?, IR, BS}	$28\,750 \pm 3\,906$	2.92 ± 0.34	-5.00 ± 0.92	-7.00 ± 0.50	0.68 ± 0.01
010	CD–32 12943	0.15	59	1.51	B2V	$23\,510 \pm 1\,427$	4.08 ± 0.16	-2.29 ± 0.34	-4.25 ± 0.35	0.71 ± 0.01
014	CD–32 12929	0.20	69	1.40	B3VI ^{BE?}	$19\,247 \pm 670$	4.28 ± 0.08	-1.48 ± 0.12	-2.71 ± 0.31	0.73 ± 0.01
047	CD–32 12954	0.39	71	1.84	A8V	$7\,652 \pm 176^a$	4.32 ± 0.01^a	2.40 ± 0.15^a	2.29 ± 0.15^a	1.54 ± 0.07
057	CD–32 12946 ^{dd}	0.49	70	1.73	A2V	$9\,573 \pm 322$	4.36 ± 0.10	0.77 ± 0.23	1.08 ± 0.43	1.07 ± 0.05
076	CD–32 12908	0.18	65	1.49	B3Ve ^{Em}	$20\,473 \pm 822$	4.23 ± 0.09	-1.62 ± 0.20	-3.26 ± 0.29	0.72 ± 0.01
083	CD–32 12919	0.13	66	1.35	B1V ^{BE?}	$25\,644 \pm 1\,062$	4.18 ± 0.10	-2.28 ± 0.28	-4.41 ± 0.26	0.70 ± 0.01
085	CD–32 12910	0.26	91	2.01	F0V ^{BE, mk}	$7\,300 \pm 163^a$	4.34 ± 0.01^a	2.70 ± 0.30^a	2.61 ± 0.30^a	1.62 ± 0.02
100	CD–32 12924	0.10	74	1.27	B0V ^{BEc, BE2}	$29\,500 \pm 1\,590$	4.22 ± 0.05	-2.90 ± 0.37	-5.39 ± 0.51	0.68 ± 0.01

Notes. The symbol : is used to indicate extrapolated values. g is the stellar surface gravity given in cm s^{-2} . (^{dd}) Stars with a SBD. (^{mk}) Spectral types derived using the MK-system. (^{BE}) Spectroscopic Binary. (^{BE2}) Double line spectroscopic binary. (^{BEc}) Eclipsing binary. (^{BS}) Blue straggler star. (^{Em}) Emission line star. (^{IR}) Star with infrared excess. (^{MA}) Magnetic Ap star. (^V) Variable star. (^{VB}) Visual binary. (^a) Values interpolated from Cox & Pilachowski (2000). (^m) Value calculated in this work, using a relation between Φ_b^0 and $(B - V)_0$ given by Moujtahid et al. (1998).

Table 14. NGC 6383: Physical parameters and distance to the stars.

ID	Other	m_v	$E(B - V)$	$(m_v - M_v)_0$	AD	p	$\log \mathcal{L}_\star$	M_\star	age
Eggen/The/ Lloyd Evans	designation	[mag]	[mag]	[mag]	[arcmin]	[%]	[\mathcal{L}_\odot]	[M_\odot]	[Myr]
001	CD–32 12935	5.68	0.53 ± 0.01	9.4 ± 0.3	1.47	76.5	5.4 ± 0.3	35 ± 5	3 ± 0.4
002	CD–32 12931	10.43	0.66 ± 0.01	10.5 ± 0.3	2.76	1.9	3.6 ± 0.3	9 ± 1	3 ± 3
003	CD–32 12927	10.30	0.49 ± 0.02	7.3 ± 0.2^{pm}	3.61	0.0	1.3 ± 0.2	2 ± 0.1	409 ± 206
006	CD–32 12921	9.07	0.51 ± 0.01	12.5 ± 0.9^{pm}	5.49	0.0
010	CD–32 12943	10.00	0.60 ± 0.01	10.4 ± 0.3	6.64	3.2	3.7 ± 0.3	9 ± 1	9 ± 6
014	CD–32 12929	9.85	0.50 ± 0.01	9.8 ± 0.1	2.22	55.2	3.0 ± 0.3	6 ± 0.5	6 ± 7
047	CD–32 12954	9.99	0.23 ± 0.05	6.9 ± 0.2^{pnm}	6.81	0.0	0.9 ± 0.2	2 ± 0.1	458 ± 459
057	CD–32 12946 ^{dd}	10.64	0.49 ± 0.04	8.3 ± 0.2	4.68	0.2	1.4 ± 0.3	2 ± 0.1	164 ± 173
076	CD–32 12908	9.83	0.58 ± 0.01	9.7 ± 0.2	11.71	76.5	3.2 ± 0.3	7 ± 1	9 ± 7
083	CD–32 12919	9.53	0.49 ± 0.01	10.3 ± 0.3	7.03	5.5	3.8 ± 0.3	10 ± 1	3 ± 3
085	CD–32 12910	9.53	0.27 ± 0.02	5.0 ± 0.3^{pnm}	10.28	0.0	0.8 ± 0.3	1.5 ± 0.1	467 ± 536
100	CD–32 12924	8.97	0.40 ± 0.01	10.6 ± 0.4	6.20	1.1	4.1 ± 0.3	13 ± 2	2 ± 2

Notes. m_v values obtained from SIMBAD database. (^{dd}) Stars with a SBD. (^{pm}) Probable member star. (^{pnm}) Probable non-member star.

Table 15. NGC 6530: Stellar fundamental parameters from the BCD system. Nomenclature according to Walker (1957), and Kilambi (1977).

ID	Other	D	λ_1	Φ_b	S.T	T_{eff}	$\log g$	M_v	M_{bol}	Φ_b^0
Walker/ Kilambi	designation	[dex]	[Å]	[μ]		[K]	[dex]	[mag]	[mag]	[μ]
007	HD 164 794	0.01	9	1.10	O4V((f)) ^{so,V,BE,Em}	42 857 ± 1 000 ⁿ	3.92 ± 0.30 ⁿ	-5.50 ± 0.50 ⁿ	-9.41 ± 0.34 ⁿ	0.61 ± 0.03 ^m
009	HD 164 816	0.05	...	0.66	O9III ^{mk,V,BE2,p,Em}	31 846 ± 1 000 ⁿ	3.53 ± 0.30 ⁿ	-5.25 ± 0.50 ⁿ	-8.29 ± 0.50 ⁿ	0.93 ± 0.03 ^m
032	GEN# +2.65300032	0.14	60	0.81	B2V ^{V,Em}	24 964 ± 1 539	4.08 ± 0.15	-2.33 ± 0.33	-4.49 ± 0.36	0.70 ± 0.00
042	HD 315 032	0.08	58	0.95	B0IV ^{V,Hα,Be}	31 688 ± 2 368	3.90 ± 0.30	-3.74 ± 0.54	-6.23 ± 0.42	0.68 ± 0.00
043	HD 315 026	0.09	66	0.86	B0V ^{V,Vv,ST}	29 534 ± 1 271	4.15 ± 0.11	-2.92 ± 0.40	-5.82 ± 0.41	0.68 ± 0.00
045	HD 164 865 ^{dd}	0.14	21	2.56	B4Ia ^{V,Hα}	15 208 ± 1 636	2.44 ± 0.07 ^a	-6.20 ± 0.03 ^a	-7.15 ± 0.15 ^a	0.76 ± 0.03
055	HD 315 023	0.10	78	0.80	B0VI ^{V,Em}	28 882 ± 1 511	3.94 ± 0.00 ^a	-4.00 ± 0.64 ^a	-7.16 ± 0.64 ^a	0.69 ± 0.00
056	CD-24 13829	0.07	64	1.05	B0V ^{V,Vv,BE2,Em}	33 494 ± 1 836	4.06 ± 0.20	-3.86 ± 0.36	-6.70 ± 0.50	0.67 ± 0.01
059	HD 315 033	0.13	70	1.19	B1V ^{V,p}	26 656 ± 1 163	4.21 ± 0.08	-2.41 ± 0.29	-4.71 ± 0.38	0.70 ± 0.01
060	LSS 4615	0.08	62	1.04	B0V ^{V,Vr,Em}	31 948 ± 1 922	4.03 ± 0.20	-3.54 ± 0.43	-6.24 ± 0.36	0.67 ± 0.01
061	ALS 16976	0.13	66	0.92	B1V ^{V,Em}	26 483 ± 1 034	4.17 ± 0.10	-2.41 ± 0.29	-4.61 ± 0.39	0.70 ± 0.00
065	HD 164 906 ^{dd}	0.03	51	1.27	O ^{V,Vr,BE,p,Be}	35 655 ± 3 828:	2.97 ± 0.36:	-5.70 ± 0.88	-8.24 ± 0.70:	0.66 ± 0.01:
066	CD-24 13831	0.10	...	0.95	B1V ^{V,He,Em}	25 450 ± 4 550 ^a	3.94 ± 0.00 ^a	-3.23 ± 0.77 ^a	-5.98 ± 0.77 ^a	0.62 ± 0.02 ^m
068	CD-24 13830	0.08	60	1.70	B0Ve ^V	31 622 ± 2 282	3.97 ± 0.27	-3.47 ± 0.60	-5.98 ± 0.44	0.68 ± 0.01
070	ALS 18783	0.13	73	0.67	B2V ^{Em}	26 044 ± 1 632	4.25 ± 0.06:	-2.17 ± 0.32:	-4.44 ± 0.51:	0.70 ± 0.01
073	HD 315 031	0.07	56	1.08	B0IV ^{Vv,ST}	33 249 ± 2 996	3.81 ± 0.39	-3.92 ± 0.61	-6.62 ± 0.42	0.68 ± 0.01
076	HD 315 024	0.08	58	0.83	B0IV ^{Em}	32 189 ± 2 391	3.89 ± 0.30	-3.76 ± 0.48	-6.20 ± 0.44	0.68 ± 0.01
080	CD-24 13837	0.05	42	0.82	O9Ib ^{Vr,Em}	25 977 ± 4 032	2.71 ± 0.14:	-6.22 ± 0.89:	-7.79 ± 0.81	0.68 ± 0.01
085	HD 164 933	0.07	...	1.16	B0III ^{Vv,mk}	29 732 ± 1 000: ⁿ	3.49 ± 0.30: ⁿ	-5.11 ± 0.50: ⁿ	-7.95 ± 0.50: ⁿ	1.09 ± 0.03 ^m
086	CD-24 13840	0.17	88	0.70	B2V ^{BE2,BEe,Em}	20 900 ± 3 225 ^a	3.94 ± 0.00 ^a	-2.45 ± 0.60 ^a	-4.80 ± 0.60 ^a	0.62 ± 0.02 ^m
093	HD 315 021	0.08	62	1.06	B0V ^{Vv}	31 086 ± 1 967	4.05 ± 0.20	-3.43 ± 0.53	-5.91 ± 0.41	0.68 ± 0.01
100	HD 164 947	0.16	77	1.04	B2VI ^{VB,V,BE,Be}	22 166 ± 1 268	3.94 ± 0.00 ^a	-2.45 ± 0.60 ^a	-4.80 ± 0.60 ^a	0.72 ± 0.01
...	LSS 4627	0.13	64	0.58	B1V	26 483 ± 1 241	4.14 ± 0.11	-2.57 ± 0.31	-4.64 ± 0.33	0.70 ± 0.00

Notes. The symbol : is used to indicate extrapolated values. g is the stellar surface gravity given in cm s^{-2} . (^{dd}) Stars with a SBD. (^{so}) Spectral types derived using “The Galactic O-Star Spectroscopic Survey” (Sota et al. 2011). (^{mk}) Spectral types derived using the MK-system. (^{BE}) Spectroscopic binary. (^{BE2}) Double line spectroscopic binary. (^{BEe}) Eclipsing binary. (^{Be}) Known Be star. (^{Em}) Emission line star. (^{H α}) Star with emission in H α . (^{He}) Helium star. (^p) Chemically peculiar star. (ST) Triple system. (^V) Variable star. (^{VB}) Visual binary. (^{Vr}) Radial velocity variable. (^{Vv}) Probable variable like Vega star. (^a) Values interpolated from Cox & Pilachowski (2000). (^m) Value calculated in this work, using a relation between Φ_b^0 and $(B - V)_0$ given by Moujtahid et al. (1998). (ⁿ) Stellar parameter given by Martins et al. (2005).

Table 16. NGC 6530: Physical parameters and distance to the stars.

ID Walker/ Kilambi	Other designation	m_v [mag]	$E(B - V)$ [mag]	$(m_v - M_v)_0$ [mag]	AD [arcmin]	p [%]	$\log \mathcal{L}_\star$ [\mathcal{L}_\odot]	M_\star [M_\odot]	age [Myr]
007	HD 164 794	5.93	0.33 ± 0.02	10.4 ± 0.5^{pm}	8.78	0.0	5.7 ± 0.4	54 ± 13	1 ± 0.6
009	HD 164 816	7.09	...	11.5 ± 0.5^{pm}	8.25	12.4	5.3 ± 0.4	31 ± 10	5 ± 0.8
032	GEN# +2.65300032	10.37	0.08 ± 0.01	12.5 ± 0.3	4.53	0.0	3.8 ± 0.3	10 ± 1	7 ± 5
042	HD 315 032	9.18	0.20 ± 0.01	12.3 ± 0.5	4.14	0.3	4.6 ± 0.4	186 ± 4	4 ± 2
043	HD 315 026	9.01	0.13 ± 0.01	11.5 ± 0.4	7.84	12.4	4.2 ± 0.3	14 ± 1	3 ± 2
045	HD 164 865 ^{dd}	7.74	1.23 ± 0.02	10.1 ± 0.1^{pm}	11.10	0.0	4.8 ± 0.2	17 ± 3	10 ± 2
055	HD 315 023	10.07	0.09 ± 0.01	13.8 ± 0.6^{pm}	7.95	0.0	4.6 ± 0.4	17 ± 2	7 ± 1
056	CD–24 13829	9.08	0.29 ± 0.01	12.1 ± 0.4	2.22	4.8	4.7 ± 0.4	19 ± 3	3 ± 2
059	HD 315 033	8.90	0.34 ± 0.01	10.3 ± 0.3^{pm}	5.10	0.0	3.9 ± 0.3	10 ± 1	2 ± 2
060	LSS 4615	9.65	0.27 ± 0.01	12.4 ± 0.4	1.60	0.1	4.5 ± 0.3	17 ± 2	3 ± 2
061	ALS 16976	10.28	0.17 ± 0.01	12.2 ± 0.3	1.61	1.3	3.8 ± 0.3	10 ± 1	3 ± 3
065	HD 164 906 ^{dd}	7.45	0.46 ± 0.01	11.7 ± 0.9	2.02	71.6
066	CD–24 13831	10.17	0.25 ± 0.02	12.6 ± 0.8	1.45	0.0	4.2 ± 0.5	12 ± 2	12 ± 6
068	CD–24 13830	9.75	0.76 ± 0.01	10.9 ± 0.6	2.00	0.0	4.5 ± 0.4	17 ± 4	3 ± 2
070	ALS 18783	10.48	...	11.8 ± 0.4	1.58	80.8	3.7 ± 0.3	10 ± 1	2 ± 3
073	HD 315 031	8.31	0.30 ± 0.01	11.3 ± 0.6	0.71	1.0	4.8 ± 0.5	22 ± 10	3 ± 2
076	HD 315 024	9.55	0.11 ± 0.01	12.0 ± 0.5	2.11	0.0	4.6 ± 0.4	19 ± 5	3 ± 2
080	CD–24 13837	9.39	0.11 ± 0.01	15.3 ± 0.9^{nm}	1.77	0.0
085	HD 164 933	8.70	0.04 ± 0.02	13.7 ± 0.5^{pm}	11.87	0.0
086	CD–24 13840	9.60	0.06 ± 0.02	11.9 ± 0.6	0.89	39.9	3.7 ± 0.4	9 ± 1	24 ± 1
093	HD 315 021	8.59	0.28 ± 0.01	11.2 ± 0.5	1.99	0.2	4.4 ± 0.4	15 ± 2	3 ± 2
100	HD 164 947	8.87	0.24 ± 0.01	10.6 ± 0.6	2.49	0.0	3.8 ± 0.4	9 ± 1	19 ± 4
...	LSS 4627	11.37	...	13.1 ± 0.4^{nm}	196.64	0.0	3.9 ± 0.3	10 ± 1	3 ± 3

Notes. m_v values obtained from SIMBAD database. The distances of the stars with negative color gradients were determined using the distance modulus assigned to the cluster. ^(dd) Stars with a SBD. ^(pm) Probable member stars. ^(nm) Non-member stars.